Ambiente & Água - An Interdisciplinary Journal of Applied Science
ISSN 1980-993X – doi:10.4136/1980-993X
www.ambi-agua.net
E-mail: ambi.agua@gmail.com

Seasonal variations in residence time and water age in the Mundaú-Manguaba Estuarine Lagoon System, AL (Brazil)

ARTICLES doi:10.4136/ambi-agua.2887

Received: 12 Sep. 2022; Accepted: 26 Jan. 2023

Lucas de Carvalho Ferreira[1*]; Monica Pertel[1]; Paulo Cesar Colonna Rosman[2]

[1]Programa de Engenharia Ambiental. Escola Politécnica e Escola de Química. Universidade Federal do Rio de Janeiro (UFRJ). Avenida Athos Silveira, n° 149, CEP: 21945-970, Rio de Janeiro, RJ, Brazil. E-mail: monicapertel@poli.ufrj.br
[2]Programa de Engenharia Naval, Oceânica e Costeira. Área de Engenharia Costeira e Oceanográfica. Instituto Alberto Luis Coimbra de Pós Graduação de Engenharia, Universidade Federal do Rio de Janeiro (UFRJ), Avenida Athos Silveira, n° 149, CEP: 21945-970, Rio de Janeiro, RJ, Brazil. E-mail: pccrosman@ufrj.br
[*]Corresponding author. E-mail: lc_ferreira@poli.ufrj.br

ABSTRACT

The Characteristic Hydraulic Times (CHT), called Residence Time (R_T) and Water Age (W_A), were analyzed in the Mundaú-Manguaba Estuarine Lagoon System (MMELS – AL, Brazil), using the SisBaHiA® – Environmental Hydrodynamics Base System, for two scenarios: wet season, from May to July 2018; and dry season, from October to December 2018. The hydrodynamic modelings appropriately represented water level variations measured in the lagoons. The analysis of residual currents revealed how hydrodynamic circulation was affected by seasonal variations, and provided essential information to understand the results of the R_T and W_A simulations. This study deepened the knowledge regarding the R_T of the water masses inside the lagoons, and reinforced how river discharges significantly influence their export, which resulted, considering the spatial scope, in much smaller R_T in the wet season compared to the dry season. The W_A analysis added new and significant knowledge about water renewal, from a different perspective, and as yet little-explored in the study region. Among the results obtained, the most relevant refer to the dry season, in which it was found that the “oldest” waters in the Mundaú L. occurred near the southeast region, while in the Manguaba L., in the vicinity of the central region. Both regions were confirmed as the places that present the most critical trophic state index in each lagoon, showing that W_A is a CHT that indicates the regions most conducive to more critical trophic states.

Keywords: Mundaú-Manguaba lagoons, residence time, water age.

Variações sazonais no tempo de residência e na idade da água no Complexo Estuarino Lagunar Mundaú-Manguaba, AL (Brasil)

RESUMO

Os Tempos Hidráulicos Característicos (THC) denominados Tempo de Residência (T_R) e Idade da Água (I_A) foram analisados no Complexo Estuarino Lagunar Mundaú-Manguaba (CELMM – AL, Brasil), através do SisBaHiA® – Sistema Base de Hidrodinâmica Ambiental, para dois cenários: período chuvoso, de maio a julho de 2018; e período seco, de outubro a dezembro de 2018. As modelagens hidrodinâmicas representaram adequadamente as variações de nível d'água observadas nas lagunas. As análises das correntes residuais revelaram como a circulação hidrodinâmica foi afetada pelas variações sazonais, e forneceram informações essenciais para compreender os resultados das simulações de T_R e da I_A. Este estudo aprofundou os conhecimentos em relação ao T_R das massas de água no interior das lagunas, e reforçou como as descargas fluviais influenciam significativamente a exportação das mesmas, o que resultou, considerando a abrangência espacial, em T_R bem menores no período chuvoso, em comparação ao período seco. As análises da I_A agregaram novos e significativos conhecimentos quanto à renovação das águas, por meio de uma perspectiva diferente, e ainda pouco explorada na região de estudo. Dentre os resultados obtidos, os mais relevantes se referem ao período seco, no qual constatou-se que as águas mais "velhas", na laguna Mundaú, ocorreram próximo da região sudeste, enquanto na laguna Manguaba, nas proximidades da região central. Ambas as regiões foram confirmadas como os locais que apresentam os índices de estado trófico mais crítico, em cada laguna, evidenciando que a I_A é um THC que indica os locais mais propícios a estados tróficos mais críticos.

Palavras-chave: idade da água, lagunas Mundaú-Manguaba, tempo de residência.

1. INTRODUCTION

The characteristic hydraulic times (CHT) are useful parameters for analyzing the mixing and renewal of the water masses in the domain of interest, based on hydrodynamic circulation (Monsen *et al.*, 2002; Aguilera *et al.*, 2020; Bocaniov and Scavia, 2018; Gao *et al.*, 2020; Pham Van *et al.*, 2020). They are usually adopted in studies of water bodies under strong influence of anthropic actions, especially with regard to the release of industrial and domestic effluents. This is because the water quality of an aquatic system is directly related to the quality of the affluent waters, as well as the water's residence time (Du and Shen, 2016; Roversi *et al.*, 2016; Marsooli *et al.*, 2018; Liu *et al.*, 2020).

In the literature, CHT has several denominations, among them: Residence Time (R_T); Flushing time; Turnover Time; Hydraulic Retention Time; Times of Renewal Rates ($T_{RR\%}$), and Water Age (W_A). Usually, it is common to find different definitions, concepts, and varied application approaches for each CHT, as highlighted by Aguilera *et al.* (2020); therefore, it is essential to precisely define the methodology adopted, so that the results are correctly interpreted. Through the use of Computational Models of Environmental Hydrodynamics, specifically the Transport Models, it is possible to characterize the CHT in the water body in a spatial and temporal way; that is, in spatial terms, to identify in which regions water renewal occurs more quickly, as well as those where it occurs slowly, and in terms of renewal time in each location, which varies depending on changes in environmental forcings, such as river discharges. This approach is suitable when studying estuarine systems and reservoirs, as well as other aquatic systems that present very complex geometry, with great spatial heterogeneity and varied flow conditions in space at a given instant as well as over time (Dalazen *et al.*, 2020; Rosman, 2021).

In terms of water quality, the CHT by itself does not provide results that allow a direct judgment about it, as would be possible to obtain through water-quality modeling. However, from the values obtained, together with the knowledge of the quality of the affluent waters, it is possible to infer the susceptibility of certain places to develop water quality problems. For regions close to the rivers, i.e., which are largely renewed by them, it is easy to deduce that the water quality of this region will be strongly influenced by freshwaters. In this case, greater water renewal can mean worsening in quality, if the freshwaters are of poor quality. On the other hand, regions where renewal occurs more slowly may present more favorable conditions for eutrophication intensification, especially if the water residence time is longer than the time scales of biogeochemical processes (Knoppers *et al.*, 1991; Gao *et al.*, 2018; Zhao *et al.*, 2021).

By identifying the most vulnerable regions to pollution loads, it is possible to better define the most relevant places for monitoring and to prioritize actions to improve the environmental quality of an aquatic system in favor of water-resource management. CHT water-quality analyses have been increasingly applied. Aguilera *et al.* (2020) performed simulations of three CHTs in Patos Lagoon (RS, Brazil), namely R_T, $T_{RR\%}$, and W_A, and found that the region north and northeast of the lagoon are the more vulnerable to eutrophication, and therefore recommended monitoring these areas. Tosic *et al.* (2019) studied water renewal in the Bay of Cartagena (Colombia) under different scenarios of river input and correlated the results with possible impacts on the water quality. Qi *et al.* (2016) simulated W_A in Lake Poyang, the largest freshwater lake in China, and found a strong positive correlation between this parameter and the concentration of chlorophyll *a*, as observed by Bocaniov and Scavia (2018) in the study on the Lake St. Clair (USA-Canada). Regarding the last two studies, it is observed that the concept of W_A adopted by the authors refers to the time that a water parcel has been within the system since it entered through one of the boundaries (Monsen *et al.*, 2002). This concept is different from the one adopted in this study, as will be discussed below. Even so, the interpretation of the result is similar in that the regions that present the highest W_A are those that renew more slowly.

In view of the above, models of the SisBaHiA® – Environmental Hydrodynamics Base System – were applied to characterize the Mundaú-Manguaba Estuarine Lagoon System (MMELS – AL, Brazil). The specific objectives were:

• Implement and calibrate the hydrodynamic model for two scenarios: wet season (autumn-winter) and dry season (spring-summer);

• Analyze the characteristic hydraulic times (CHT), considering the concepts of Residence Time (R_T) and Water Age (W_A), in different sectors of the lagoon system.

This study deepens aspects of similar studies, relevant to the MMELS, among them: Larsson and Nilsson (2014); Lima (2017); Souza (2017); Brito Jr. *et al.* (2018); Cunha *et al.* (2021) and Pinheiro *et al.* (2021). Most of the cited works discuss the R_T. This work adds to the discussion, the W_A, highlighting the significant results that this CHT can provide regarding the mixing and renewal of water masses. In addition, CHT has been linked to water-quality issues. Based on the knowledge of the regions that presented the most critical trophic state index, it was verified which CHT best identified these regions, having as a principle that the places where water renewal occurs more slowly would be most conducive to more critical trophic states.

2. MATERIALS AND METHODS

2.1. Study Area

The Mundaú-Manguaba Estuarine Lagoon System (MMELS) is located in the state of Alagoas (AL), in northeastern Brazil, as shown in Figure 1. The MMELS is a natural system that encompasses two lagoons, Mundaú and Manguaba, classified as “choked lagoons”. It has communication channels with the Atlantic Ocean, and several islands and an estuarine area common to both lagoons. It has an area of just over 80 km^2, the Mundaú L. with ≈ 26 km^2 and an average depth of 1.5 m; Manguaba L. with ≈ 42 km^2 and average depth of 2.1 m. The channels are about 12 km^2 (Oliveira and Kjerfve, 1993; ANA, 2006; Brito Jr. *et al.*, 2018). The main tributary rivers to MMELS are the Mundaú R, in the lagoon of the same name, and Paraíba do Meio R., in the Manguaba L. The Mundaú R. has a drainage basin of ≈ 4120 km^2, while the Paraíba do Meio R. drainage basin is ≈ 3160 km^2. It also includes the Sumaúma R., with a drainage area of ≈ 370 km^2, which flows to the south of the Manguaba L. (ANA, 2006).

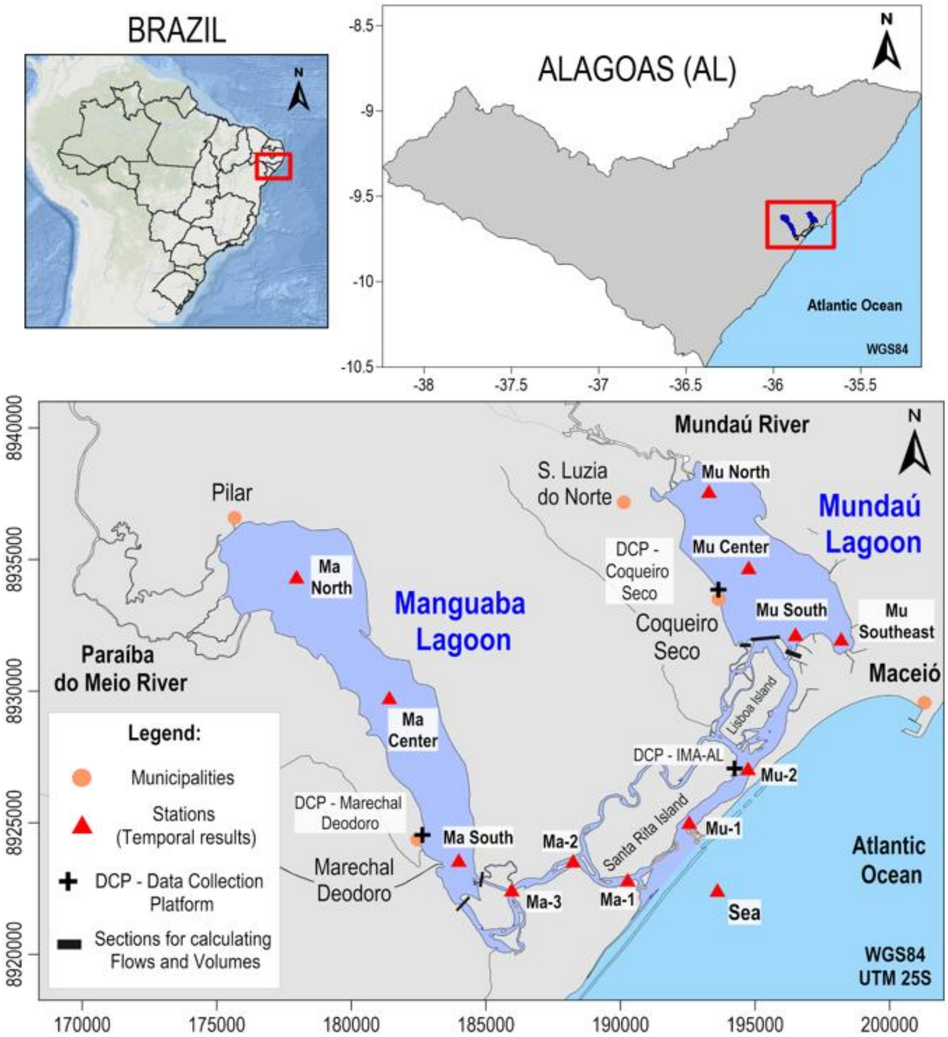

Figure 1. Location of MMELS and its main tributaries, highlighting the municipal seats, in addition to other information that will be detailed throughout the development of this study.

The climate is tropical, with a wet season in autumn-winter, and a dry season in spring-summer. The wet season occurs from April to August, with the wettest quarter in May-June-July. The dry season, from October to February, with the driest quarter in October-November-December (Barros *et al.*, 2012). According to the National Institute of Meteorology – INMET, from 1961 to 2018, the annual mean rainfall was 1913 mm, with June presenting the highest average, 329 mm, while November the smallest, 43 mm. The discharges of the Mundaú and Paraíba do Meio R. vary considerably between the wet and dry seasons, with values above 1000 $m^3 s^{-1}$ and lower than 5 $m^3 s^{-1}$ (ANA, 2021).

In the drainage basins of MMELS, the population is ≈ 1151000 inhabitants, according to the Brazilian Institute of Geography and Statistics – IBGE (2010). In the capital, Maceió, it is estimated, from the IBGE (2021), that around 31% of the population, i.e., ≈ 319000 inhabitants are found in the areas of contribution to MMELS, located mainly on the east and south margins of the Mundaú L. The economic activities carried out in the basins are responsible for a significant portion of pollution in the lagoons, mainly due to agriculture, especially sugarcane monoculture, with the use of fertilizers and agrochemicals; sugar and alcohol producing plants, which generate effluents with high organic load; the Chemical and Petrochemical industries, with oil, gas and rock salt exploration in areas close to the lagoons; and agricultural activities, among others (ANA, 2006; Cotovicz Jr. *et al.*, 2012; Lima, 2017).

In urban areas, sanitation is precarious, so that part of the sewage is released without treatment in the watercourses and lagoons, further deteriorating the quality of its waters (Tamano *et al.,* 2015; ANA, 2017; Maceió, 2017; SNIS, 2019). Cotovicz Jr. *et al.* (2012) evaluated the trophic state of MMELS by applying the ASSETS model (Assessment of Estuarine Trophic Status), TRIX (Trophic Index) and three other trophic state indices, and found that both lagoons are eutrophic, mainly due to great nutrient input. The Mundaú L. presented moderate eutrophic state while in the Manguaba L. the state was highly trophic. The authors indicate a trend of little improvement in relation to the conditions presented in that study. In the lagoons, especially in the Mundaú L., fishing is an activity of great relevance, being practiced by hand and in an extractive way. Among the species found – crustaceans, mussels and fish – the mussel *Mytella charruana* stands out, known locally as “sururu”, which, besides being a source of income for thousands of residents of the surrounding area, is still characterized as a typical food of the region. Over the last few years, the exploitation of fishing resources has been hampered, among other factors, by the increase in pollution (Coutinho *et al.*, 2014; Ribas *et al.*, 2019).

2.2. Computational Model Adopted

The computer simulations were carried out using SisBaHiA®, a professional system of computational models developed at COPPE/UFRJ. In the midst of the various computational tools available, such as MIKE 21/3 (DHI, 2021) and Delft3D (Deltares, 2021), the SisBaHiA® was adopted due to its suitability to the study's purposes and its proven applicability and efficacy in the environmental modeling of estuarine systems, in addition to its accessibility. Examples of applications include the work developed by Lima (2016), Silva (2019), Aguilera *et al.* (2020); Dalazen *et al.* (2020) and Cunha *et al.* (2021). SisBaHiA® is widely used in the development of studies and projects focused on water resources and environmental management, as verified in the sections "Applications - Projects" and "Research - Theses", in http://www.sisbahia.coppe.ufrj.br/. The models used are briefly described below. Details of the models that make up SisBaHiA®, as well as their mathematical formulations, can be found in the Technical Reference of SisBaHiA® (Rosman, 2021), on the same site.

2.2.1. Hydrodynamic Model (HM)

The HM, called FIST3D (Filtered in Space and Time 3D*)*, adopts space-time filtering techniques optimized for natural water bodies. FIST represents a modeling method in which the definition of resolvable and non-resolvable scales (turbulence) of flow modeling is based on filtering techniques similar to those employed in Large Eddy Simulation (LES) (Rosman, 1997). FIST3D solves the complete Navier-Stokes equations with approximation of shallow waters, i.e., considering the hydrostatic pressure approach. The spatial discretization is optimized for natural aquatic systems and is preferably done via biquadratic quadrilateral finite elements, but quadratic triangular finite elements or the combination of both can also be used. Temporal discretization is performed via an implicit finite difference scheme, with second order truncation error (Rosman, 2021). The HM is composed of a 2DH module, vertically averaged, and a 3D module. According to Oliveira and Kjerfve (1993), ANA (2012c), Lima (2017) and Cunha *et al.* (2021), the Mundaú and Manguaba L. are shallow, subject to the action of tides and frequent winds coming from E to SE. Because of that, the water column is mostly well mixed. Based on this, a modeling with vertically averaged variables is suitable. Horizontal density gradients were considered in the HM, through the simulation of salinity and temperature, using the Water Quality and Eutrophication Model (WQM). In this way, the salinity and temperature models were executed coupled to the HM, i.e., they were computed simultaneously by SisBaHiA®. The hydrodynamic modeling with density gradient has as variables the water level, the velocity components, the density as a function of salinity and temperature, and the advective-diffusive transport equations for salinity and heat (temperature).

The WQM, in mathematical and numerical terms, is similar to the advective-diffusive Eulerian Transport Model (ETM) integrated in the vertical, and can count, depending on the reactivity of the constituent, with kinetic reactions of production and consumption through physical, biological and chemical processes (Rosman, 2021).

2.2.2. Eulerian Transport Model (ETM) and Lagrangian Transport Model (LTM)

The ETM and LTM are models of advective-diffusive transport with kinetic reactions. Such models also adopt space-time filtering techniques. The ETM aims to simulate the transport and the average water column concentration of passive scalars, which do not interfere with the hydrodynamics. This model was used to simulate the W_A. The LTM can be used to simulate the scalar transport of substances mixed in the water column, through the observation of the trajectory of particles in the modeling domain. This model was used to simulate the R_T.

2.3. Modeling Steps

2.3.1. Digital Terrain Modeling

The modeling domain was delimited from Google Earth Pro® images, referring to the year 2018. Subsequently, the discretization of the modeling domain was performed at SisBaHiA® by means of a mesh of biquadratic quadrilateral and quadratic triangular finite elements. The mesh has 3227 finite elements, 3093 of which are quadrilateral and 134 triangular, resulting in a total of 14533 calculation nodes. Of this total, 10665 are internal nodes, 3803 belong to the land boundary, and 67 to the oceanic open boundary. The mesh area corresponds to 102.57 km^2. The bottom topography was characterized with bathymetric data from several sources, among them: National Institute of Waterway Research (Portobrás and INPH, 1985); Petróleo Brasileiro S.A. (Petrobrás, 2011); National Water and Sanitation Agency (ANA, 2012a); Geological Service of Brazil (CPRM, 2019); Nautical Charts (NC) from Directorate of Hydrography and Navigation (DHN) of the Brazilian Navy, namely: Port of Maceió NC Nº. 901 (Brasil, 1977) and Proximity to the Port of Maceió NC Nº. 920 (Brasil, 1977). From the bathymetry, it is highlighted that the area of the free surface of the water, at mean sea level (MSL), which is 1.16 m, is equivalent to 102.27 km^2, while the volume, 403.14×106 m^3. At MSL, the average depth is equal to 3.94 m.

In the wet season, the bathymetry of the mouth was inferred from Google Earth Pro® images, in which it was possible to identify the deepest stretches and the shallowest stretches with sandbanks. Morphological relationships of width and average depth (Buckmann, 2019) were used, correcting the averages according to the images. The bathymetry adopted proved to be adequate, as evidenced by the good fit between measured and simulated levels in the lagoons and in the Mundaú L. channel, as mentioned in Section 3.1. This fact proves that the volumetric exchanges between the lagoons and the sea are correct. This would not occur with inadequate geometry of the embouchure. Note that the water level measurement stations are represented in Figure 1, with the name of DCP (Data Collection Platform). For reefs located in front of the mouth, for which information was not available, the heights of their crests were also estimated using Google Earth Pro®, together with tidal data. Figure 2, on the left, presents the bathymetric map, whose values are referenced to the Reduction Level (RL) of the DHN – CN Nº 901, which indicates the mean sea level (MSL) at 1.16 m above the RL. The same figure, on the right, shows the hypsometric curves of Elevation x Area x Volume, for each lagoon. Note that the minimum and maximum elevations were obtained from hydrodynamic simulations, as mentioned in Section 3.1.

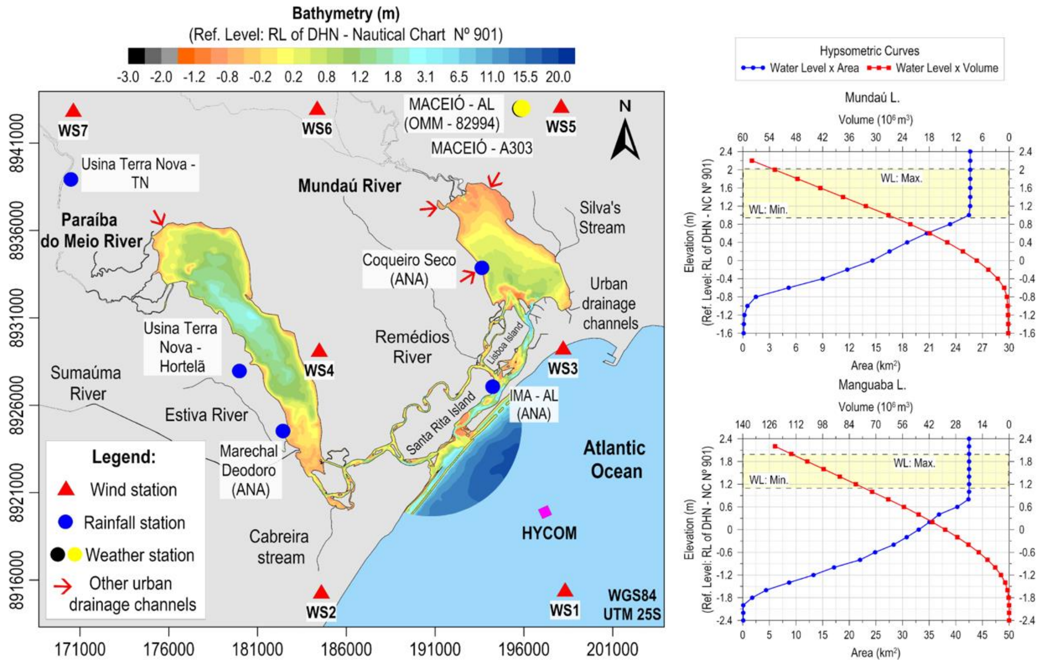

Figure 2. On the left, the bathymetry adopted in the modeling domain, referenced to Nautical Chart Nº 901 of the DHN. The wind, rainfall, weather and HYCOM stations are also presented. On the right, the hypsometric curves of Elevation x Area x Volume for each lagoon.

The characterization of the type of bottom material is essential to calculate the bottom friction stresses. The coefficient of friction at the bottom depends on the type of sediment, as presented in Section 3.2.3.2 in the Technical Reference of SisBaHiA® (Rosman, 2021). At the bottom of the lagoons, fine sediments, silt and clay predominate, for which the equivalent bottom roughness amplitude (ε) of 0.005 m was adopted. According to ANA (2012b), the region near the mouth of the Mundaú R. has a significant presence of medium and coarse sand (0.03 m ≤ ε ≤ 0.04 m). A little to the south of this region, there is the presence of fine sand (ε = 0.01 m). To the south, close to the communication channel, there is coarse sand. In the channels, medium and coarse sand predominates. In the Manguaba L., close to the mouth of the Paraíba do Meio R., there are coarse and medium sands. In the southern region, close to the mouth of the Sumaúma R. and near the communication channels, the predominance of medium sands was considered. In the communication channels of the lagoons, including the inlet, the predominance of medium to coarse sands was considered (Portobrás and INPH, 1985; Oliveira and Kjerfve, 1993; ANA, 2006; 2012b). In the coastal region, the predominance of coarse sand was adopted, while in the reefs, a material similar to a bedrock was considered, with ε = 0.12 m.

2.3.2. Modeling and Environmental Data Scenarios

To show the effects of seasonality on hydrodynamic circulation, two scenarios were considered:

- Wet season (autumn-winter): from 05/01/2018 00h00 to 08/01/2018 00h00
- Dry season (spring-summer): from 10/01/2018 00h00 to 01/01/2019 00h00

Before starting the simulation of the wet season, the model was previously run (HM + WQM), in a pre-modeling of the wet season, with a duration corresponding to 30 days, in order to create appropriate initial conditions for the respective season. This action allowed the model to adequately represent the large river discharge that occurred at the beginning of the wet season. In this pre-modeling, a “cold” start of the HM was carried out, with the water level homogeneous and equal to 1.16 m (MSL), also considering velocities equal to zero. The initial condition of the salinity and temperature models are presented later. The months of August and September were also simulated, in order to consider the continuity and evolution of the W_A, as well as salinity and temperature, for dry season simulation. Some settings adopted in the HM, ETM, WQM and LTM are presented. In HM, the time step was 7.5 s, while in ETM, WQM and LTM, 60 s. In the HM, the temporal results were recorded in a time intervals of 15 min – the same interval as the data from DCP stations –, while for the spatial ones, 30 min. was used. As for the ETM and WQM, the values were, respectively, 30 min and 1 h. For the LTM, the results were recorded in the interval of 1 h. In HM, the maximum Courant number was 14.5 and the average was 1.3. Regarding turbulent dispersion, the turbulent dispersion tensors are calculated according to Equation 1:

$$\begin{aligned} D_{xx} &= D_L \cos^2\varphi + D_T sen^2\varphi \\ D_{xy} &= D_{yx} = D_L D_T sen\varphi \cos\varphi \\ D_{yy} &= D_L sen^2\varphi + D_T \cos^2\varphi \end{aligned} \quad (1)$$

Where D_L and D_T are, respectively, the coefficients in the longitudinal and transverse directions and φ is the angle between the current direction and the x axis. The D_L and D_T coefficients are parameterized according to Elder (1959), based on Equation 2:

$$\begin{aligned} D_L &= \alpha 5.93 u_* H \\ D_T &= \beta 0.15 u_* H \end{aligned} \quad (2)$$

Where α and β are calibration parameters, u_* is the characteristic friction velocity and H is the height of the water column, which varies in space and time. α = β = 1 was adopted. For more details, see the Technical Reference of SisBaHiA® (http://www.sisbahia.coppe.ufrj.br/).

The forces considered in the hydrodynamic modeling are presented below:

Sea level boundary condition

The tidal series were generated in SisBaHiA®, from the harmonic constants of the Port of Maceió, provided by the National Oceanographic Database. Figure 3 presents the sea level variations adopted in the respective seasons. In the study region, the tides are classified as semidiurnal and present a mesotidal regime. From May to July, the mean level was 1.24 m, and the maximum tidal range was 2.31 m. From October to December, the values were 1.08 m and 2.36 m, respectively.

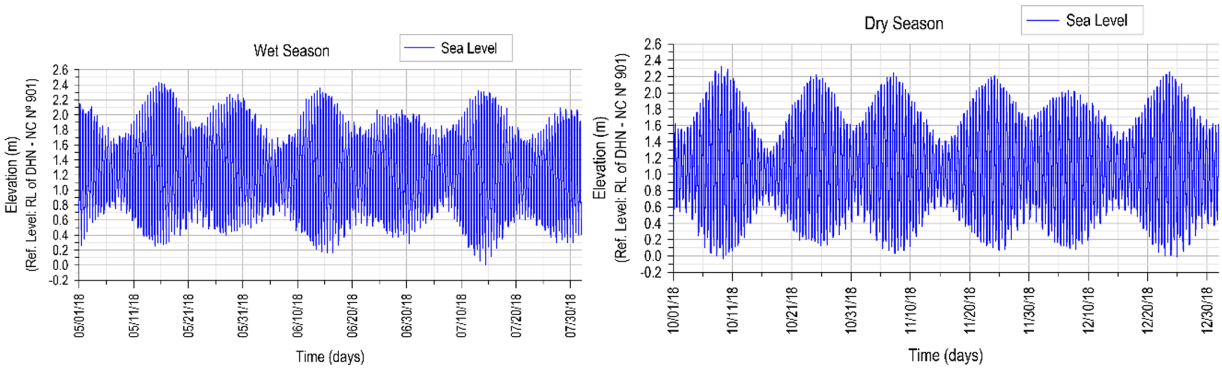

Figure 3. Time series of free surface elevation adopted in the oceanic open boundary conditions, for the wet season, on the left, and for the dry season, on the right.

Coastal currents

In order to represent the effects of coastal drift currents dissociated from astronomical tides in the simulation, the Differential Mean Level (DML) was adopted in the oceanic open boundary (OB) conditions. DML is a way of inducing currents by creating a gap in the free surface of the water. The values calculated for the DML are added to the values of level variation already prescribed for each node of the OB. To calculate this difference, it is necessary to define the pivot axis (PA) of the DML and import a reference time series, called the Differential Mean Level Generator Series (DMLGS). The PA is a straight line, and was created with a direction perpendicular to the coastline, crossing a point in the central region of the OB. Basically, the PA divides the OB into two regions, in which on one side an increment in the level is added, while on the opposite side this value is subtracted. At the point where the AP crosses the segment of OB, the increment is equal to zero, i.e., this is the neutral point. The module and signal of this increment are obtained from the DMLGS, also considering a scale factor (calibration) and the distance from the node to the PA. Note that the module and the signal are directly associated with the magnitude and direction of the induced currents.

The DMLGS was generated from the following steps: first, a series of velocity components U (East) and V (North) were obtained from the Hybrid Coordinate Ocean Model (HYCOM), with a temporal resolution of 3 h for the point illustrated in Figure 2. After that, from the components obtained at different depths, the average velocities in the water column were calculated and then the magnitude and direction of the currents. Finally, the decomposition of the average velocity vectors was performed, in order to calculate the component parallel to the coastline, i.e., SW-NE direction. In summary, the magnitude and direction of the currents, present in the DMLGS, were mathematically translated into coastal currents in the OB, via DML. The currents were not calibrated and validated, due to the absence of measured data. Details regarding the mathematical formulations can be found in Section 3.5.1.3 in the Technical Reference of SisBaHiA® (Rosman, 2021). Based on the HYCOM data, the predominant direction of the currents was SW, 78% of the time in the wet season and 99% in the dry season. What is expected, since in May, June and July there are more cold fronts, which induce currents to NE.

River discharges

The discharges were obtained in two ways. The first via HidroWeb Portal, from the National Water and Sanitation Agency (ANA, 2021), and the second through the estimation of discharges to water courses and urban drainage channels. Through the HidroWeb Portal, the daily mean discharges were obtained from the stations present in the Mundaú R. (Code: 39770000; Name: Fazenda Boa Fortuna; Lat.: 9.4672º S; Long.: 35.8597º W; Drainage area: 3560 km^2) and the Paraíba do Meio R. (Code: 39870000; Name: Atalaia; Lat.: 9.5067º S; Long.: 36.0228º W; Drainage area: 2600 km^2). As these stations are located upstream of the lagoons, the discharge values were adjusted considering correlations between the drainage areas of the stations and the drainage areas to the lagoons. Figure 4 shows the hydrographs with increased discharges for the simulations. In the same figure, the bar graphs compare the monthly mean discharges in the year 2018 and historical, available in each station. For the Mundaú R., from 1974 to 2017, while for Paraíba do Meio R., from 1977 to 2017.

Note, in relation to Mundaú R., that during the wet season simulated monthly mean discharges were well below the historical values, except in May. A similar scenario occurred in Paraíba do Meio R., but in this case, the discharges in this season were all below the historical data. In the dry season, both stations presented values below historical data. In 2018, October and November had monthly mean discharges close to the minimum discharge rate Q95% – discharges exceeded 95% of the time – which is 4.71 $m^3\ s^{-1}$ for the Mundaú R., and 2.16 $m^3\ s^{-1}$ for the Paraíba do Meio R. In this case, was obtained for the Mundaú R., 4.89 $m^3\ s^{-1}$ and 4.02 $m^3\ s^{-1}$, respectively. For the Paraíba do Meio R., 2.66 $m^3\ s^{-1}$ and

2.95 $m^3 s^{-1}$, respectively.

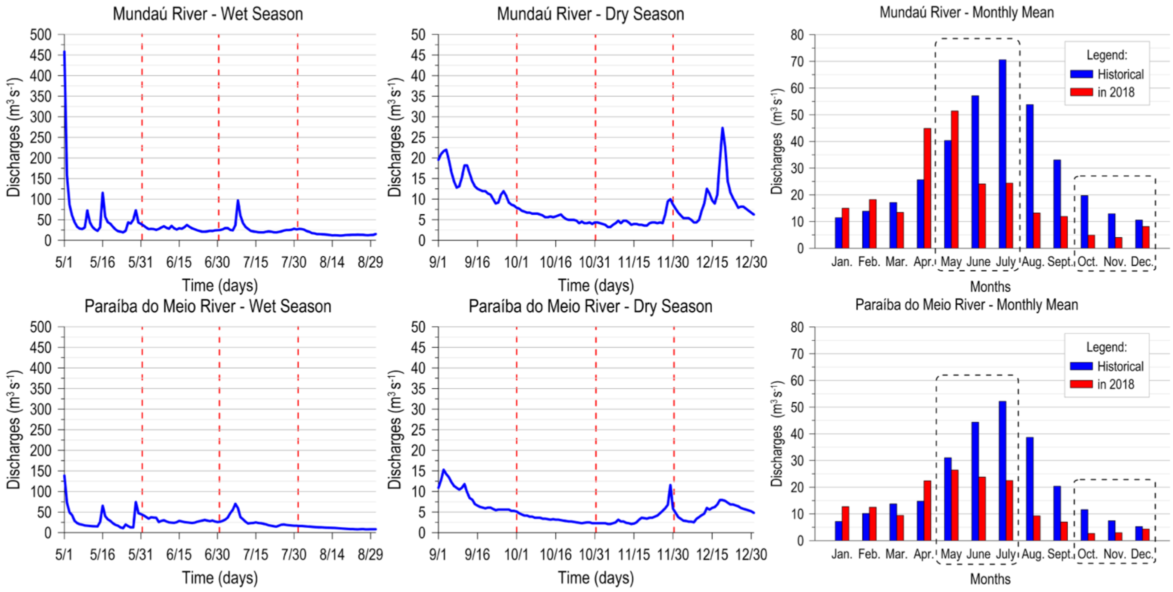

Figure 4. On the left and center, hydrographs with increased discharges of the Mundaú and Paraíba do Meio R. On the right, the historical and the year 2018 monthly mean discharges, referring to the respective stations.

At the beginning of the wet season there was a daily mean discharge of ≈ 460 $m^3 s^{-1}$ to Mundaú L., a value that exceeded the mean of annual maximums, whose estimated value is 432 $m^3 s^{-1}$. An event of this magnitude significantly influenced the renewal and exportation of the water masses of this lagoon, as will be discussed in the results. The discharges of the other watercourses were composed of the sum of two contributions. The first refers to the estimation of inflows of sewage to MMELS, coming from the urban areas around the lagoons. The second contribution came from the drainage discharges generated in the sub-basins of the respective urban areas. In this case, the discharges were estimated using the Modified I-Pai-Wu Method, based on the study of São Paulo (1999), considering monthly mean values. Figure 2 shows all the rivers and urban drainage channels considered in the simulations; however, Table 1 presents, in summary form, the relevant discharges for this study. Note that the discharges of the Sumaúma and Remédios R. were estimated from Oliveira and Kjerfve (1993) and ANA (2006).

Table 1. Summary of monthly mean discharges (drainage + sewage), presented by sub-basins.

Sub-basins	Area (km^2)	Discharges ($m^3 s^{-1}$): Drainage + Sewage					
		Wet season			Dry season		
		May	Jun.	Jul.	Oct.	Nov.	Dec.
Silva's Stream	12.8	0.378	0.330	0.349	0.100	0.189	0.185
Maceió (South and Southeast Area – Mundaú L.)	11.3	0.543	0.471	0.499	0.123	0.257	0.251
Sumaúma R.	371.9	6.555	4.316	4.203	0.646	0.615	1.055
Estiva R.	30.5	0.349	0.247	0.359	0.026	0.097	0.127
Remédios R.	46.7	1.311	0.863	0.841	0.129	0.123	0.211

Winds

The wind data were provided by the global atmospheric reanalysis model ERA-5, from the

European Centre for Medium-Range Weather Forecasts – ECMWF, with a temporal resolution of 3 h. In order to consider the wind acting in a varied way in space, a total of seven stations were adopted, as shown in Figure 2, from which the model produced, by interpolation, the wind field acting in the entire modeling domain. It is convenient to adopt these wind stations, as this avoids considering the data from the MACEIÓ-A303 (INMET) station acting uniformly in space, which would mean saying that the wind velocity is the same throughout the modeling domain, which probably does not reflect reality. Note that the data from the station MACEIÓ-A303 (INMET) are represented by the reanalysis data, as they were absorbed by the ERA-5 model. As an example, Figure 5 shows the wind roses for the WS1 and WS6.

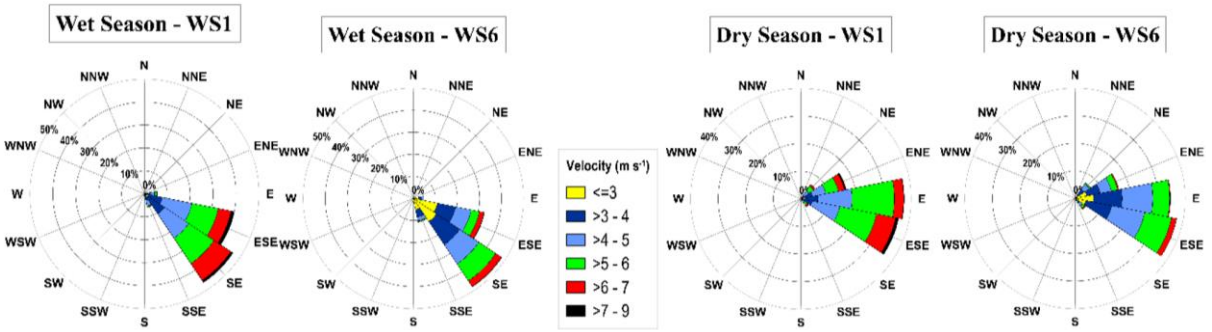

Figure 5. Wind roses for the respective seasons, in reference to WS1 and WS6, as shown in Figure 2.

The study region is under the trade winds regime. In the May, June and July quarters, the prevailing wind in WS1 was from the SE, with a frequency of 46%, followed by the ESE, with 40%. The latter presented the highest intensity, 8.5 m s^{-1}. In WS6, similarities were observed regarding the origin of the winds, and differences in relation to frequencies and intensities, since in this station the SE wind had a frequency of 48%, while the ESE, 33 %. The latter presented the highest intensity, 7.2 m s^{-1}. In the October, November and December quarters, the prevailing wind in WS1 was from the E, followed by the ESE, both with frequencies close to 37%. The latter presented the highest intensity, 7.6 m s^{-1}. In WS6, the ESE and E frequencies were also very similar, with emphasis on the prevailing ESE wind, reaching a maximum intensity of 6.9 m s^{-1}. Details regarding the mathematical formulations used in the calculation of wind friction stresses on the free surface of the water are found in Section 3.2.3.1 of the Technical Reference of SisBaHiA® (Rosman, 2021).

Rainfall and Evaporation

In the simulations, rainfall was considered acting in a variable way in time and varied in space, while evaporation was considered as variable in time and uniform in space. Daily rainfall data was considered, which were extracted from five stations, as shown in Figure 2, managed by the State Secretariat for the Environment and Water Resources of Alagoas (SEMARH-AL). July was the wettest month, with a mean accumulated rainfall of 180 mm, considering all stations, while October was the driest, with 3 mm. The daily evaporation data were acquired from the MACEIÓ-AL (OMM - 82994) station, from INMET. Regarding these, July had the lowest monthly evaporation, with ≈ 64 mm, while December had the highest, with ≈ 100 mm.

Salinity and Temperature

In the Salinity Model, the value of 0 psu (practical salinity unit) was adopted as a boundary condition (BC) for freshwater inlets. In the oceanic open boundary (OB), the data came from HYCOM, extracted from the same location shown in Figure 2. From the salinity profile, with a temporal resolution of 3 h, the mean salinity in the water column was calculated, which was inserted into the models. In the wet season, the mean values ranged between 36.4 and 36.8 psu, while in the dry season, between 36.5 and 36.7 psu. Regarding the initial condition adopted in the pre-modeling of the wet season, the value of 4.5 psu for Mundaú L. was considered homogeneously, while for Manguaba L., 3 psu was used, and 14.5 psu for the communication channels. In the Temperature Model, the BC for the rivers were acquired from the same fluviometric stations already mentioned. In the wet season, values ranged between 25.9 and 28.1°C, while in the dry season, between 28.3 and 30.4°C. At the oceanic OB, the same procedure described in relation to salinity was carried out. In the wet season, the mean values ranged between 26.0 and 28.4°C, while in the dry season, between 26.6 and 28.2°C. The other relevant data, namely, solar radiation, air temperature and relative air humidity, were obtained from the weather station MACEIÓ-A303 (INMET), shown in Figure 2. Regarding the initial condition adopted in the pre-modeling of the wet season, the average value between the temperatures of the main rivers – Mundaú and Paraíba do Meio – and of the sea, i.e., the value of 29°C, was considered in the lagoons and communication channels. It is observed that the salinity and temperature models were not calibrated and validated, due to the absence of measured data.

2.3.3. Residence Time (R_T) and Water Age (W_A) Simulations

Residence Time (R_T)

The R_T is usually defined as the time water remains in a given fluid compartment before being transported out of that compartment. The methodology for determining the R_T, as a spatially variable function, is described below. The R_T simulation begins with the filling of the compartment, i.e., the domain of interest, with several neutral particles, which do not occupy space. These particles symbolize centroids of water mass parcels and are passively transported by currents. Note that the model assigns each particle its own number, and the initial position and time of its launch into the compartment are linked to it. Throughout the simulation, the model follows the trajectory of each particle, step by step. While the particle remains inside the compartment, its lifetime increases and is counted. When the particle leaves the compartment, its lifetime becomes the R_T, assigned to the particle's initial position. At the end of the simulation, if the particle has not left the compartment, the R_T at the particle launch position will be equal to the simulation time. In this study, the compartment corresponded to the lagoons, with the control sections equivalent to those adopted to calculate the series of resulting flows and volumes, as shown in Figure 1. In all, the compartment was filled with 143825 particles, distributed in a regular grid of 15×15 meters. The simulation time corresponded to 92 days, in the respective seasons. In this model, the total reflection of the particles, i.e., null absorption, was adopted as a boundary condition.

Water Age (W_A)

Based on the Technical Reference of SisBaHiA® (Rosman, 2021), W_A represents the average age of water in a given sector of the water body. In other words, on average, how long the waters of a given location are within the modeling domain. For example, regions near river and sea entrances will have shorter ages, as they are regions that always receive “new” waters, while areas further away from these locations tend to have “older” waters. To calculate the W_A, the model considers an age-marking passive substance, C (x, y, t), which undergoes first-order decay, with a constant rate $K_d > 0$. The effects of losses or mass gains are disregarded. As an example, consider a volume of water well mixed with the initial concentration C_0 of such a substance. The time variation of the concentration of the age-marking substance, C(t), is given by Equation 3:

$$\frac{dC}{dt} = -K_d C \tag{3}$$

Whose analytical solution leads to Equation 4:

$$C(t) = C_0\, exp(-K_d t) \therefore t = \frac{-ln(C/C_0)}{K_d} \quad (4)$$

Knowing the initial concentration C_0 and a concentration C recorded later, it is possible to determine the decay time, t, elapsed between the initial instant of simulation and the instant of recording C. The decay time, t, represents the "W_A", at the time of registration of C. The K_d, whose unit is the inverse of time, was related to the equivalent time called T_{90}, i.e., the time required for 90% concentration decay, equivalent to an order of magnitude. By adopting $C/C_0 = 0.1$, $K_d = -\ln(0.1)/T_{90}$ is calculated. In the simulation, at a given time and place, as a consequence of the turbulent advective-diffusive transport mechanisms, the value of the function W_A (x, y, t) symbolizes an average of the mixture of waters of different ages, being expressed by Equation 5:

$$W_A(x,y,t) = ln(\,C(x,y,t)/C_0)\,\frac{T_{90}}{ln(0.1)} \quad (5)$$

In the conception of this model, it was adopted that, at the initial instant, t_0, all the water in the modeling domain was homogeneous with C (x, y, t_0) = C_0 = 1.0, i.e., W_A, at the initial instant, is equal to zero in all locations, because ln(1) = 0. Note that this initial condition was adopted in the simulation performed before the wet season, with the objective of creating appropriate initial conditions for the respective season. Usually, the initial condition of $W_A = 0$ in the entire modeling domain is adopted at the beginning of the simulation of the period of interest, as can be seen in the study by Pinheiro *et al.* (2021). A negative point of starting from a homogeneous condition is the time spent for the W_A to reach a condition of dynamic equilibrium, given as a function of environmental forcings. Thus, to avoid starting the wet season with a homogeneous condition, the value of $W_A = 0$ was previously adopted, in pre-modeling, with a duration corresponding to 30 days. In addition, after the wet season, the W_A was also simulated in August and September, in order to consider its evolution over time, and consequently generate initial conditions for the dry season.

For "new" waters entering the modeling domain by rivers, by sea and by rainfall, a concentration value equal to 1 was assigned, i.e., they have $W_A = 0$. It is worth mentioning that the concentration value is independent of variations in inflows, as well as the water quality. Over time, the initial waters and the waters that enter the domain are mixed and transported, which causes a decrease in the value of C in each location, due to the decay process and, consequently, generates an increase in W_A. With regard to the T_{90}, Rosman (2021) recommends that the value be close to the simulation time, in order to ensure numerical accuracy. Thus, T_{90} = 92 days was adopted, equivalent to the simulation time in each season. To understand the results, consider that at a given time and place, the value of W_A = 20 days, this means that the waters at that time and place are, on average, 20 days in the modeling domain. Based on the study by Aguilera *et al.* (2020), the W_A can be related to the CHT called Times of Renewal Rates ($T_{RR\%}$), as it estimates the time required to renew at least 50% of the waters in a given region. As an example, if a given region, over a given period, has an average W_A = 5 days, it can be interpreted, given the environmental forcings of this period, that it would take, on average, 5 days to renew at least 50% of the waters of this region.

3. RESULTS AND DISCUSSIONS

3.1. Hydrodynamics Analysis

Figures 6 and 7 show, respectively, the time series of elevations measured and simulated in the lagoons for July in the wet season, and for October in the dry season. Note that the July results expose the model calibration, performed in the wet season, while the October results express its validation. Analyzing the results, the good coherence between measured and simulated data stands out, in which it was obtained, from the linear regression of the data from both seasons, coefficients R^2 = 0.98, for the correlation between the stations "Mu-2" and "DCP IMA-AL", as well as for the stations "Ma South" and "DCP Mal. Deodoro." For the stations "Mu Center" and "DCP Coq. Seco", R^2 = 0.99 was obtained.

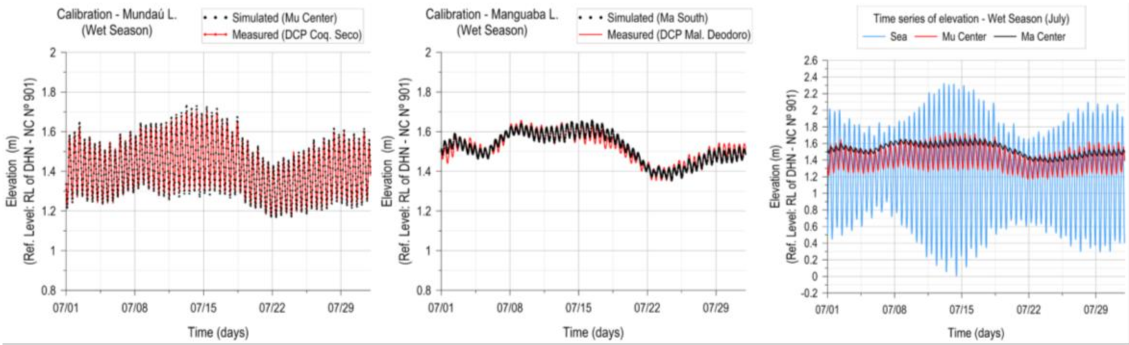

Figure 6. On the left and center, the time series of elevations measured and simulated in the lagoons, for July, in wet season, representing model calibration. On the right, the time series of elevation in the stations "Sea", "Mu Center" and "Ma Center", for the same month.

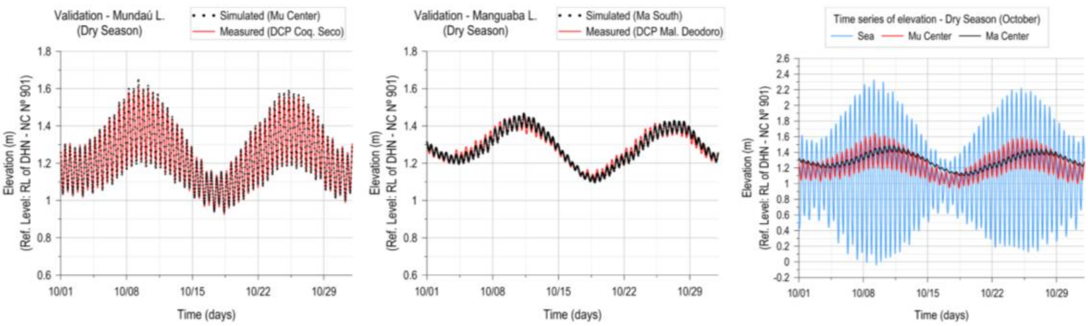

Figure 7. On the left and center, the time series of elevations measured and simulated in the lagoons, for October, in the dry season, representing model validation. On the right, the time series of elevation in the stations "Sea", "Mu Center" and "Ma Center", for the same month.

When analyzing the time series of elevation for the stations "Sea", "Mu Center" and "Ma Center", Figure 7, the great attenuation of the tides inside the lagoons is evident. The attenuation is exemplified in Figure 8. In the selected spring tidal cycles, there is a tidal attenuation of 81% for the "Mu Center" station, and ≈ 97% for the "Ma Center" station. The main cause of this is the great loss of energy by friction in the communication channels of the lagoons, mainly for the Manguaba L. At "Mu-1" station, the evident asymmetry of the tidal curve can be seen. Asymmetry increases by reducing the ratio between the semidiurnal and quarter-diurnal harmonic constants, e.g., M2/M4, at each location. For example, in the coastal region the M2/M4 ratio is 80.5, in the "Mu-2" station it drops to 8.1, and in the "Mu Center" station it is equal to 10. Similarly, in the "Ma-2" station M2/M4 is equal to 7, and at the "Ma Center" station, 7.7.

Regarding the water levels in the lagoons, in reference to RL of the DHN – CN Nº 901, the maximum level in the "Ma Center" station was 1.99 m, while in "Mu Center", 2.02 m. These values are directly related to the discharge peaks of the Paraíba do Meio and Mundaú R., occurring at the beginning of the wet season. During this season, the average level of the Mundaú L. was 1.45 m, corresponding to an average depth of 1.51 m, and an average volume of 38.79×10^6 m^3. As for the Manguaba L., the values were, respectively, 1.57 m, 2.26 m and 96.18×10^6 m^3. In the dry season, the lowest level was observed, at station "Ma Center" equal to 1.10 m, while at station "Mu Center", 0.94 m, as shown in Figure 7. During this season, the average level of the Mundaú L. was 1.24 m, corresponding to an average depth of 1.30 m, and an average volume of 33.32×10^6 m^3. As for the Manguaba L., the values were, respectively, 1.30 m, 2.00 m and 84.87×10^6 m^3.

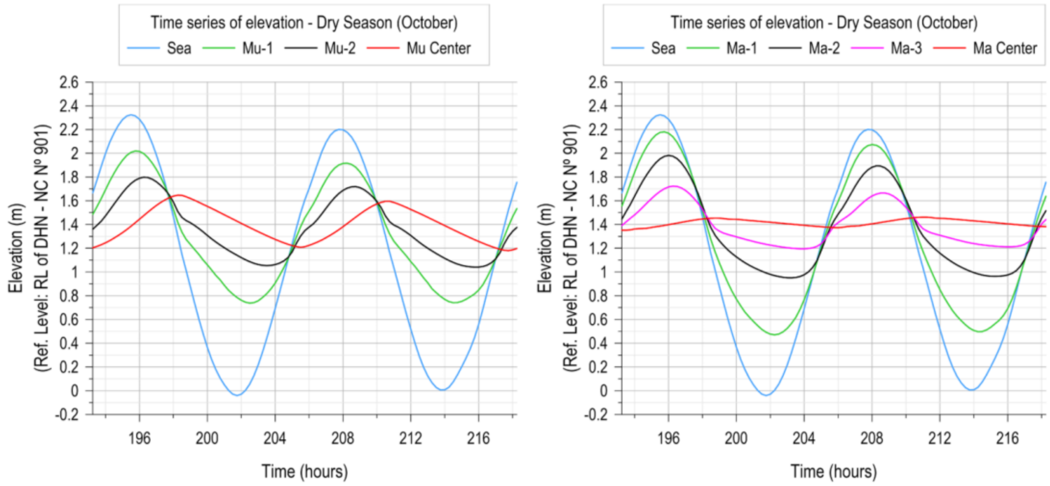

Figure 8. Time series of elevation in October, in the time interval from 193.25 h (10/09/2018 01h15) to 218.25 h (10/10/2018 02h15), for the stations "Sea", "Mu-1", "Mu-2" and "Mu Center", on the left; and "Sea", "Ma-1", "Ma-2", Ma-3" and "Ma Center", on the right.

In general, the hydrodynamic circulation in the Mundaú L. is mainly governed by the tides, being strongly influenced at times of high river discharges. Winds are also relevant, especially during the dry season, contributing to the generation of vortices, i.e., circulatory cells in the lagoon, as will be presented in the analysis of residual currents. In this lagoon, the highest currents speeds occurred close to the communication channel, reaching a maximum of 1.4 m s^{-1}. In contrast, the southeast region presented very low speeds. At “Mu Southeast” station, the maximum was 0.017 m s^{-1}. At the “Mu Center” station, the average speed was equal to 0.04 m s^{-1}, reaching a maximum of 0.1 m s^{-1}, as a result of the large discharge of the Mundaú R. In the Manguaba L., the tides are considerably reduced. Thus, river discharges and winds play a very important role in hydrodynamic circulation. In general, the highest speeds occurred in the south region, close to the communication channels. At “Ma South” station, the maximum was ≈ 0.2 m s^{-1}. In the northern region, however, very low speeds were observed. At “Ma North” station, the maximum was 0.025 m s^{-1}, and occurred at the beginning of the wet season. At the “Ma Center” station, the average speed was 0.015 m s^{-1}, reaching a maximum of 0.036 m s^{-1}, in a spring flood tide in October. The hydrodynamic circulation patterns were characterized through maps of isolines and vectors of currents, which are found in Annex I. It is observed that the currents refer to the average in the water column. In the wet season, a spring cycle was selected, in the time interval from 05/17/2018 05h00 to 05/17/2018 17h30, and in the dry season, a neap cycle, in the time interval from 10/16/2018 09h00 to 10/16/2018 21h30. The moments of high water (HW), mid-ebb tide (MET), low water (LW) and mid-flood tide (MFT), relative to the water level at the “Ma-1” station, were highlighted. It is observed that in the cycle selected for the wet season, the wind came from the SE, with an average speed of 3.4 m s^{-1}, while in relation to the dry season, it came from the ENE, with an average speed of 4.9 m s^{-1}.

Figure 9 shows the maps of isolines and vectors of residual currents, for two spring tidal cycles in the respective seasons. These currents reflect the resulting flow and are calculated based on the temporal average of the currents. To represent the wet season, the time interval from 05/16/2018 19h30 to 05/17/2018 20h30 was adopted, while the dry season, from 11/07/2018 06h00 to 11/08/2018 07h00. In reference to the wet season, it was observed in both lagoons that in general the residual currents were towards the communication channels. These results show how the hydrodynamic circulation, during the wet season, is significantly influenced by river discharges. In the selected cycle, the mean river discharge of the Mundaú R. was 91.5 $m^3 s^{-1}$, while of the Paraíba do Meio R., 43.3 $m^3 s^{-1}$. As for the wind, it came from the SE, with an average intensity of 3.4 m s^{-1}. In the Mundaú L., the residual currents intensity was higher in the west margin, due, among other reasons, to the bathymetry and proximity to the communication channels, while on the opposite margin, a greater influence of the winds was observed, directing the currents towards the north region. Note, in the southeast region, the occurrence of circulatory movements is counterclockwise. In this region, the residual currents showed a strong correlation with the direction of the winds, so that when they originated closer to E, clockwise movements were observed, while closer to SE caused counterclockwise movements. Regardless of the direction, very low residual currents intensity was observed, which can be interpreted as an indication that the mixing and water renewal occur more slowly in this region. The same can be said for the northwest region of this lagoon. In the Manguaba L., the tides were even more reduced, as a result of increased discharges of the Paraíba do Meio R. In the northern region, close to the east margin, low residual currents intensity prevailed, in addition to counterclockwise circulatory movements.

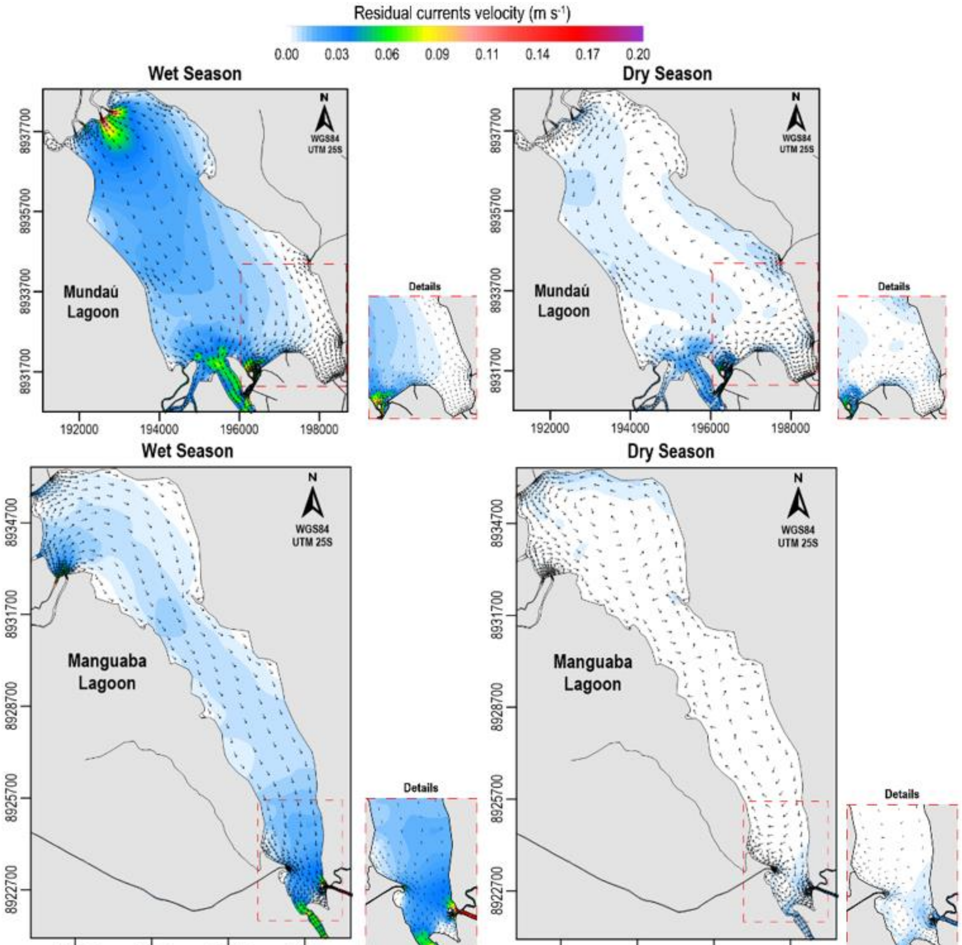

Figure 9. Maps of isolines and vectors of residual currents, on the left, for the wet season (from 05/16/2018 19h30 to 05/17/2018 20h30), while, on the right, for the dry season (from 11/07/2018 06h00 to 11/08/2018 07h00). Note that the density of vectors is much smaller than the number of calculation points, and in addition, they have the same length, in order to improve their visualization.

As for the dry season, lower residual currents intensities were observed, compared to the wet season. The decrease in river discharges made it possible to better observe the influence of the winds on the induction of currents. In the selected cycle, the mean river discharge of the Mundaú R. was 3.71 $m^3 s^{-1}$, while of the Paraíba do Meio R., 2.28 $m^3 s^{-1}$. As for the wind, it came from the E, with an average intensity of 4.4 $m s^{-1}$. In the Mundaú L, the residual currents became a large-scale, counterclockwise circular movement. Authors such as ANA (2013), Souza (2017) and Brito Jr. *et al.* (2018) also observed such a pattern, which influences the scattering of constituents present on each margin. The circulatory cell located in front of Silva's Stream stands out. The waters present in this region tend to stay longer circulating through the lagoon, which, consequently, would result in a longer R_T. In the southeast region, as in the wet season, low residual currents intensity and predominance of movements in both directions were verified. In the Manguaba L., the northern portion showed a counterclockwise movement, and this was considerably more accentuated compared to the wet season. In this region, the currents were significantly influenced by the winds, so that the further E and the more intense the winds were, the larger the circulatory cells were. On the other hand, more ESE and less intense winds attenuated the size of these cells. It can be observed that the residual currents were convergent on the west margin, and divergent on the opposite margin. Between the north and central regions of the lagoon, the residual currents, on the west margin, were towards the center of the lagoon, while on the opposite margin, towards the north. Between the central and southern regions, upstream of the mouth of the Estiva R., the residual currents also went towards the center of the lagoon by the west margin. On the opposite margin, they headed towards the communication channels. Based on these analyses, it is possible to infer that the R_T values on the east margin, between the central and southern regions, should be shorter than on the opposite margin. It is emphasized that the residual currents presented, for the respective seasons, refer to specific time intervals, and do not necessarily represent an average condition for dry or wet seasons.

Next, the tidal prisms are characterized, as well as the resulting flows and volumes of water exchanged between the lagoons and the communication channels/sea. The tidal prism is the volume of water that flows into the lagoon during the flood tide, being calculated by the product between the tide range and the lagoon's surface area. The average spring tidal prism of the Manguaba L. was 3.64×10^6 m^3 and of the Mundaú L., 10.16×10^6 m^3. The average neap tidal prism of the Manguaba L. was 1.74×10^6 m^3 and of the Mundaú L., 6.19×10^6 m^3. The area of the Manguaba L. corresponds to ≈ 1.7 times the area of the Mundaú L., however, the average tidal prism in the Manguaba L. was equivalent to only 36%, in spring tidal, and 28%, in neap tidal, of the prism in the Mundaú L. The average tidal prism in the Mundaú L. corresponded to about 23% of its average volume. In Manguaba L., the average tidal prism was only 3% of its average volume. These results demonstrate how reduced the water exchanges of this lagoon with the sea are, especially during neap tidal cycles. This explains why the waters take longer to renew in the Manguaba L. than in the Mundaú L., as will be shown in the CHT analyses.

Figures 10 and 11 show the time series of resulting flows and volumes in the respective lagoons, in the sections indicated in Figure 1. Regarding the Mundaú L., it can be noted the effect that the mean river discharge input of ≈ 460 $m^3 s^{-1}$, on the first day of the wet season, had on the flows and volumes of flooding and ebbs. A maximum ebb flow of ≈ 770 $m^3 s^{-1}$ was obtained, which resulted in the output of a volume corresponding to 20.60×10^6 m^3, equivalent to 53% of its average volume in the wet season, as can be seen in Figure 10. An event of this magnitude is, in a way, quite frequent, considering that the recurrence time calculated for this discharge was ≈ 3 years. In the Manguaba L., the discharges of the Paraíba do Meio R., on the first day, was much lower, with a daily mean value of ≈ 140 $m^3 s^{-1}$. Thus, the maximum ebb flow was 240 $m^3 s^{-1}$, with an ebb volume of 6.65×10^6 m^3, corresponding to ≈ 7% of its average volume in the wet season. Based on the information presented, the R_T and W_A are then analyzed.

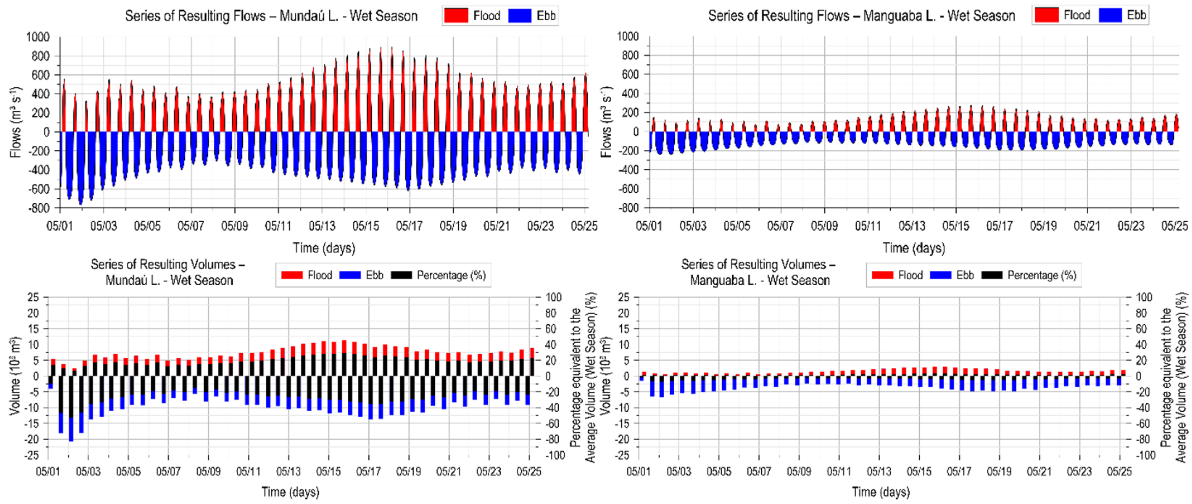

Figure 10. Time series of resulting flows, above, and resulting volumes, below, in the sections indicated in Figure 1, for the Mundaú L., on the left, and Manguaba L., on the right, in reference to the wet season.

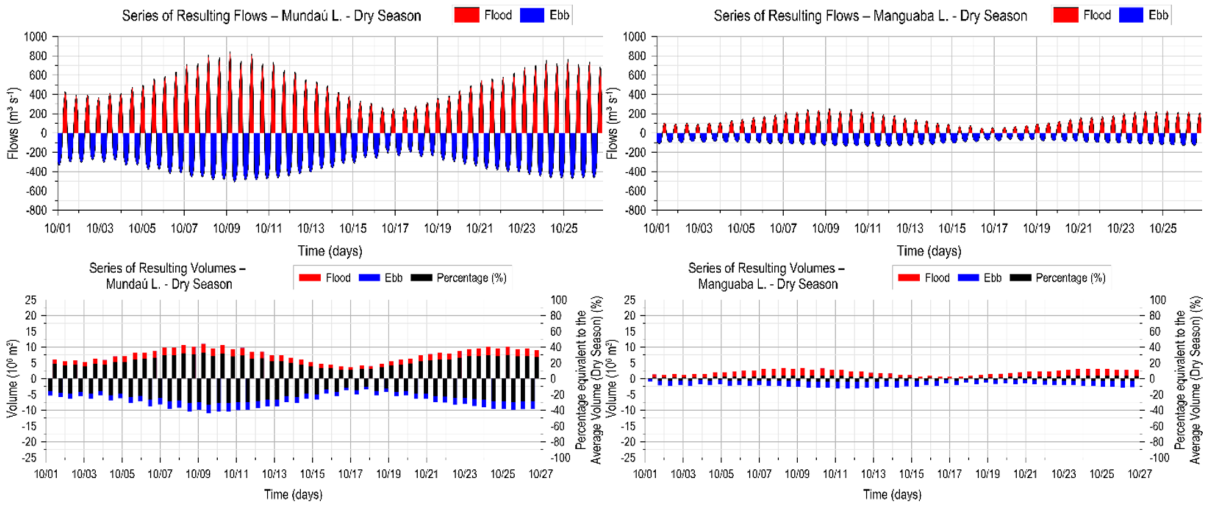

Figure 11. Time series of resulting flows, above, and resulting volumes, below, in the sections indicated in Figure 1, for the Mundaú L., on the left, and Manguaba L., on the right, in reference to the dry season.

3.2. Analysis of Residence Time (R_T)

Figure 12 shows the maps of isolines of R_T, after 92 days of simulation, in the respective seasons. In the Mundaú L., referring to the wet season, the R_T values were mostly below 2 days, i.e., the waters were quickly exported due to the great discharges of the Mundaú R. As the flow, during the ebbs, occurred preferentially near the west margin, due to the reasons mentioned in the analysis of residual currents, the values of R_T were much smaller in this margin, in comparison with the opposite margin, in which values above 45 days were obtained. Such a difference in R_T values can be explained by analyzing the trajectory of the particles initially present on the east margin. During the river discharge peak, the water masses in the east margin were driven towards the southeast region and, later, with the reduction of discharges, and by the effect of the tides and the winds, these waters were directed to the central region, around the east margin. Varying between these regions, depending on environmental forcings, water masses were progressively exported over time. In the southeast region, identified as a region in which hydrodynamic circulation does not favor water renewal, R_T of up to 60 days was obtained. Even higher values were observed in the northwest region. From these results, it can be said that, regularly, the Mundaú R. exports practically all the water present in the Mundaú L., with great efficiency during the wet seasons.

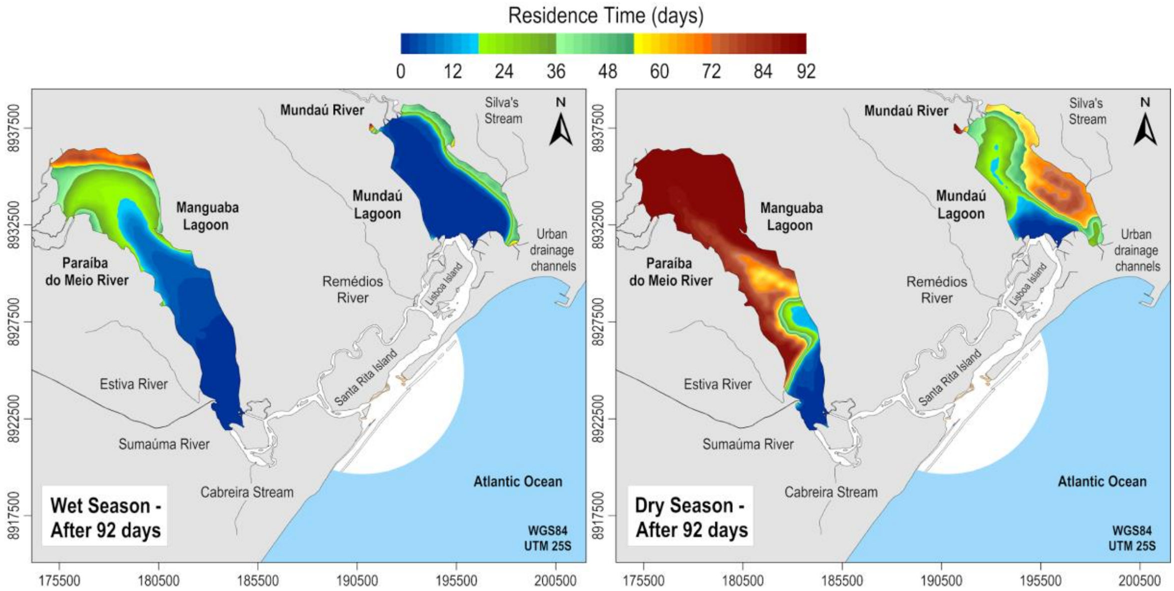

Figure 12. Maps of isolines of R_T after 92 days of simulation, for the wet season, on the left, and the dry season, on the right.

In the Manguaba L., a longitudinal gradient in R_T was observed, in a smooth way, from the south to the center, and then more accentuated, from the center to the north. In the central region, for example, the R_T was ≈ 4 days, due to the large river discharges in the first days of the simulation. The northern margin stands out, which, as it is further away from the communication channels, presents the highest R_T, above 80 days, very close to the east margin. This range of higher values can be related to the currents generated by the discharges of the Paraíba do Meio R., which pushed the water masses, initially present in this region, against the east margin. From there, these water masses moved progressively towards the communication channels, around the east margin. Through these results, the great relevance of the river discharges for the water renewal of the lagoons was clearly perceived, as pointed out by Lima (2017) and Pinheiro (2020). The results obtained corroborate the study by Pinheiro *et al.* (2021), who observed, considering average conditions of river discharges from June to August (wet season), as well as different mouth configurations, that the west margin of the Mundaú L. was renewed faster than the opposite margin, with differences greater than 50 days; and that the northern region of the Manguaba L., in the eastern portion, presented the highest R_T of this lagoon, reaching 90 days.

In the dry season, with the significant reduction in river discharges, it was observed, in some regions, a very accentuated increase in the RT. In the Mundaú L., the analysis of residual currents indicated that the region located in front of the mouth of the Silva's Stream would present high R_T, which was verified in this simulation, in which values of ≈ 80 days were obtained. In the central and eastern regions, the location with the highest R_T will vary depending on the initial condition of the simulation, as well as the environmental forcings throughout it. It can be highlighted, however, that the highest values tend to occur within the limits demarcated by the isoline of RT = 65 days. As this region is under the influence of the Silva's Stream, the input of pollution by this stream, coming from the urban region of Maceió, tends to remain for a longer time inside the lagoon, negatively affecting the water quality, mainly upstream of the mouth. In the southeast region, lower values occurred, between 26 and 50 days. There was a greater export of these water masses during the neap tide cycles, with winds coming from ENE and from E. It is noted that after export, part of these water masses, which were in the communication channel, returned to the lagoon during the flood tides. In the northwest region, the highest RT was observed in this lagoon, reaching 92 days. The patterns of hydrodynamic circulation did not favor the export of water masses from this region, in such a way that the majority was contained in the region itself. The regions that presented high RT values are in agreement with the various studies conducted, among them: ANA (2013), which obtained RT more than 80 days in the central region; Brito Jr. *et al.* (2018), who found RT above 65 days in the central and eastern part of this lagoon; and Pinheiro *et al.* (2021), which obtained, between the central and southeast regions, RT of 63 to 90 days.

In the Manguaba L., a significant portion of the water masses in the northern region remained inside the lagoon, distributed along its extension, and therefore, the R_T assigned to these water masses was equivalent to the simulation time, 92 days. Thus, it can be interpreted that the R_T of these water masses tends to be greater than 92 days. In this region, high R_T are not only due to the longer distance in relation to the communication channels, but also to the hydrodynamic circulation, which provided, due to the strong influence of the winds, a greater residence of the waters in this region, moving, preferably, counterclockwise. Cunha *et al.* (2021) also found high values in this region, with R_T exceeding 200 days. Thus, the northern region is a critical location for the input of pollution, since the polluting loads, coming, for example, from the Paraíba do Meio R. and the urban drainage channel of Pilar, tend to remain in this region for a long time, degrading the water quality in this portion of the lagoon. Based on water quality data from the Environmental Institute of Alagoas – IMA-AL, referring to the years 2012, 2013 and 2016, in reference to the mouth of the Paraíba do Meio R., it can be said that the values of Dissolved Oxygen varied between 0.4 and 13.3 mg L^{-1}, with an average of 5.2 mg L^{-1}; while those of Ammoniacal Nitrogen, from 0.01 to 0.33 mg L^{-1}, with an average of 0.07 mg L^{-1}; those of Total Phosphorus, from 0.15 to 3.1 mg L^{-1}, with an average of 1.3 mg L^{-1}. For the Biochemical Oxygen Demand, values lower than 2 mg L^{-1} up to a maximum of 14 mg L^{-1} were found.

When analyzing the central region, the R_T ranged between 57 and 92 days. The high values are associated with processes that degrade water quality, such as eutrophication, as reported, by Oliveira and Kjerfve (1993), Melo-Magalhães *et al.* (2009), Cotovicz Jr. *et al.* (2012), Brito Jr. *et al.* (2018), among others. Between the central and southern regions, it is clearly noted that the west margin presented much higher R_T, compared to the opposite margin, with differences above 85 days. By analyzing the trajectory of the particles over the dry season, it was observed that between the central and southern regions, the particles were preferentially exported along the east margin. On the opposite margin, the particles that were found upstream of the mouth of the Estiva R. were, for the most part, directed towards the center of the lagoon, along this margin. Those downstream of the mouth were, for the most part, exported in less than 20 days. This explains the large difference in the values of R_T in the vicinity of this region. For the environmental forcings adopted in the dry season, it can be inferred, based on hydrodynamic circulation, that the region close to the center, on the west margin, is susceptible to worsening water quality, as it would be influenced by the polluting loads released on this margin, both from upstream and downstream.

3.3. Analysis of Water Age (W_A)

The W_A represents, on average, how long the waters of a given location are within the modeling domain and can be interpreted as being the equivalent time to renew at least 50% of the waters in a given region. Figure 13 shows the time series of W_A, for the respective seasons, in selected stations in the lagoons. Figure 14, shows, on the left, the map of isolines of W_A for the moments of lowest W_A at stations “Mu Center” and “Ma Center”, in the wet season. In this season, May was the month that best represented a wet season, as it presented monthly mean river discharges above the annual mean. Due to this, the same figure shows, on the right, the moments of highest W_A in the lagoons in May. Figure 15, shows, on the left, the map of isolines of W_A for the moments of lowest W_A at stations “Mu Center” and “Ma Center”, in dry season. On the right, for the moments of highest W_A in the lagoons in dry season. Note in the maps, the division in a dashed line, indicating that the instants of time are distinct for each lagoon.

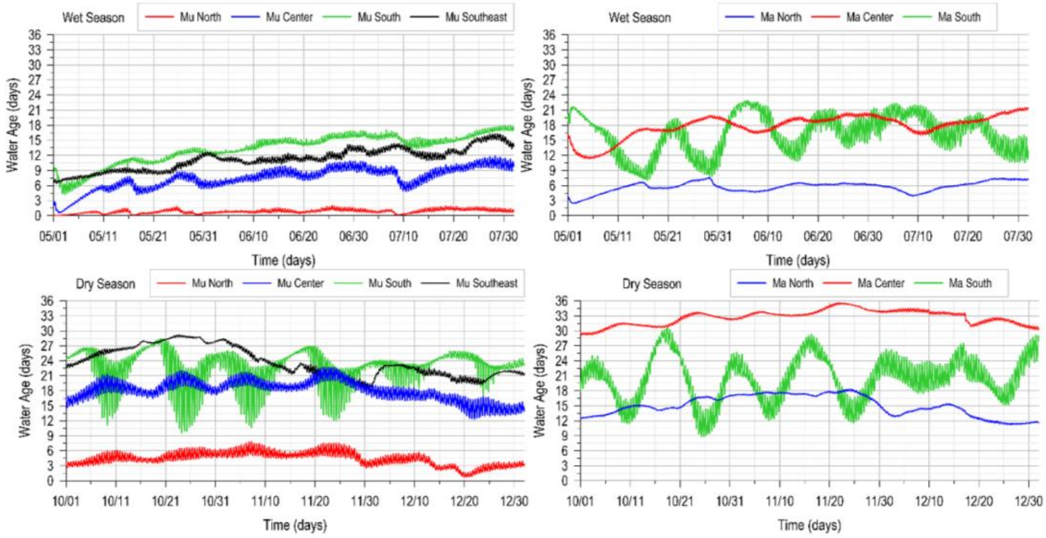

Figure 13. Time series of W_A, at the selected stations in the Mundaú L. on the left, and in the Manguaba L., on the right, in reference to the wet season, above, and the dry season, below.

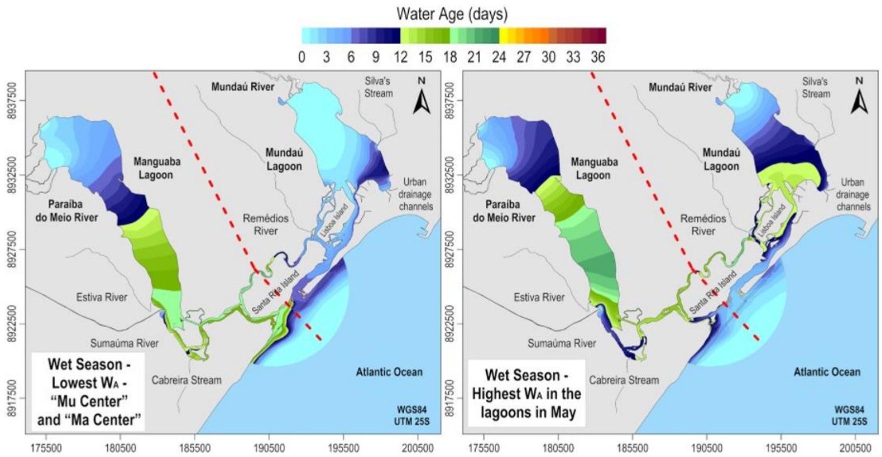

Figure 14. Maps of isolines of W_A in reference to the wet season. On the left, for the moments of lowest W_A in “Mu Center” station at time 05/02/2018 03h00; and in “Ma Center” station at time 05/05/2018 05h00. On the right, the highest W_A in May, for Mundaú L. at time 05/29/2018 06h00; and for Manguaba L. at time 05/24/2018 12h00.

In the wet season, the central region of the Mundaú L. was rapidly renewed during the first days of the simulation, due to the higher discharges of the Mundaú R. Because of this, the lowest W_A at the “Mu Center” station was 0.6 days, as shown in Figure 14 on the left. In May, the average W_A at the “Mu Center” station was ≈ 5 days. In this way, the waters that pass through this location, throughout this month, have, on average, been circulating for ≈ 5 days inside the modeling domain. It can be said that in a month with environmental forcings similar to those that occurred in May, it would take, on average, this time to renew at least 50% of the waters in the central region. As the renewal was provided in large part by the river discharges, mainly by the Mundaú R., the great influence of the quality of fresh waters on the quality of the lagoon can be inferred. For example, from the salinity simulation it was obtained for the "Mu Center" station, in reference to May, the minimum value of 0.02 psu, maximum of 0.95 psu, and temporal occurrence of 47% of waters with salinity ≤ 0.5 ups – fresh water, according to the Resolution CONAMA nº 357 of the National Environment Council. In this lagoon, the occurrence of low salinity values, in wet seasons, is mentioned by Oliveira and Kjerfve (1993), ANA (2006), Cunha *et al.* (2021), Nunes *et al.* (2021), among others.

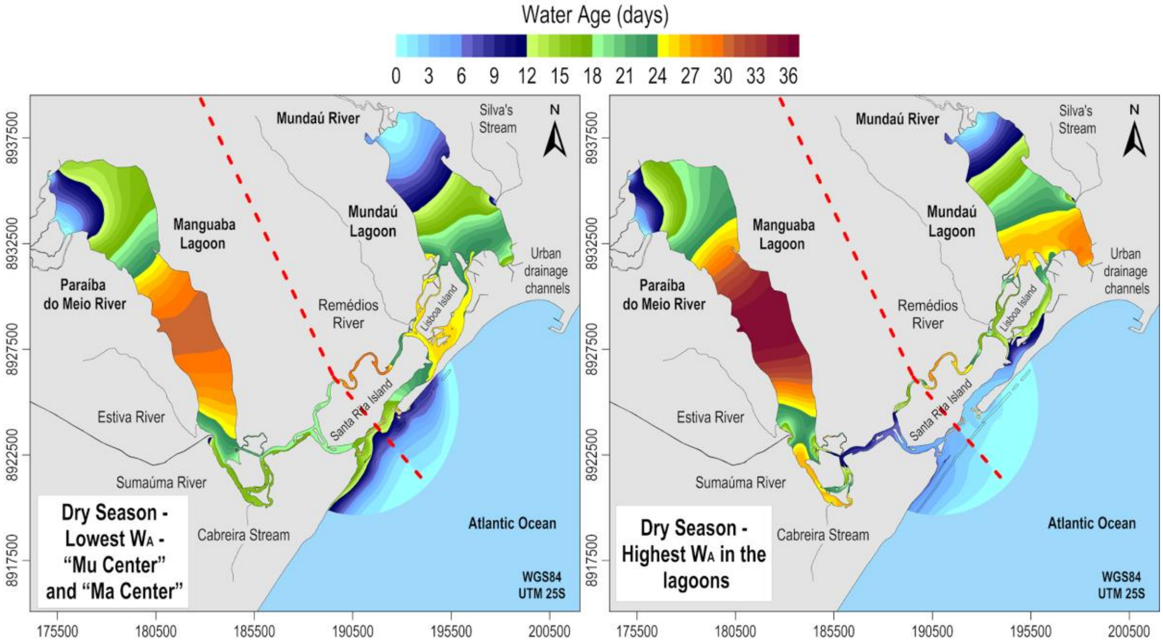

Figure 15. Maps of isolines of W_A in reference to the dry season. On the left, for the moments of lowest W_A in "Mu Center" station at time 12/22/2018 01h00; and in "Ma Center" station at time 10/02/2018 08h00. On the right, the highest W_A, for Mundaú L. at time 10/22/2018 15h00; and for Manguaba L. at time 11/20/2018 03h00.

The "Mu North" station presents $W_A \leq 2$ days, due to the proximity to the Mundaú R., which provided, in a short time, the renewal of water of this region. In the southern region, as well as in part of the communication channel, higher W_A were found compared to the rest of the lagoon, which means that the waters in these regions have been circulating in the modeling domain for a longer time. In May, the highest W_A in the "Mu South" station was ≈ 13 days. To understand the results, it should be noted that the two main sources of "new" water for this lagoon are the Mundaú R. and the sea. Thus, the regions close to these sources tend to have the lowest W_A. On the other hand, locations further away from the relevant sources of "new" water tend to have higher W_A, as they are renewed more slowly. Over time, water with high WA flows through the lagoon and communication channels, depending on the tides, river discharges, and winds. In this dynamic equilibrium, the "older" waters prevailed between the south of the lagoon and part of the communication channels. It is observed that, if there were any relevant river discharge in the southern region of the lagoon, the results would be different, with low WA values prevailing in this region. At the "Mu Southeast" station, the WA was, in general, lower than in the southern region, mainly due to the discharges of the urban drainage channels of Maceió.

In the dry season, the lowest monthly mean discharge in the Mundaú R. occurred in November, when the highest W_A values were obtained for the "Mu Center" station. From the results, it can be said that in a month with environmental forcings similar to those that occurred in November, it would take, on average, ≈ 20 days to renew at least 50% of the waters in the central region. It can be seen, in Figure 13, that the W_A in the central region tends to increase during the spring tidal cycles, due to the greater influence of the waters coming from the southern region, as well as in part of the communication channel, which have higher W_A, while in the neap tidal cycles, it tends to decrease, due to the influence of the upstream waters of lower W_A. In Mundaú L., the "Mu South" station was the one that presented the greatest W_A variation, due to the influence of both the waters coming from the sea, which provided a minimum W_A of 9.6 days, and the waters of the southeast region, when a maximum of 28.5 days was reached. At "Mu North" station, still considering November, an average W_A of 5.5 days was obtained. Despite the low discharges of the Mundaú R. that were close to the minimum, Q95%, this station reached renewal of 50% in a few days. Even under these conditions, the relevance of the Mundaú R. was perceived for the renewal of the central area of the lagoon. In this river, the presence of both industrial effluents and domestic sewage, in addition to affecting the quality of the river itself, also compromises the waters of the lagoon, especially near the mouth, as verified by ANA (2012c) and by IMA-AL, referring to the years 2012, 2013 and 2016. Based on data from the IMA-AL, referring to the mouth of the Mundaú R., it is mentioned, for example, that the Dissolved Oxygen values varied between 2 and 6.7 mg L^{-1}, with an average of 3.95 mg L^{-1}; while those of Ammoniacal Nitrogen, from 0.01 to 0.91 mg L^{-1}, with an average of 0.16 mg L^{-1}; those of Total Phosphorus, from 0.09 to 2.55 mg L^{-1}, with an average of 1.01 mg L^{-1}. For the Biochemical Oxygen Demand, values lower than 2 mg L^{-1} up to a maximum of 30 mg L^{-1} were found. In the northwest region, identified as one of the places with the highest R_T in this lagoon, a maximum W_A of ≈ 8 days was obtained. Although the water masses have remained for a long time in this region, it took just over a week to renew at least 50% of the waters.

On the east margin of the lagoon, the influence of the "new" waters from the Silva's Stream can be observed for the renewal of the very shallow region near the mouth, as shown in Figure 15. This region, therefore, tends to receive more pollution input from this stream. Such information is relevant, in view of the poor water quality of this stream, according to ANA (2012c) which found, for Dissolved Oxygen, the value of 0.25 mg L^{-1}; for Total Nitrogen, 23.35 mg L^{-1}; while for Total Phosphorus, 7.13 mg L^{-1}. In the vicinity of the southeast region, the highest values prevailed, reaching a maximum W_A of 29 days. This occurred because the waters of this region mixed more slowly with the "new" waters, mainly due to the predominance of low currents speed. This reveals that in the dry season, with similar environmental forcings, the "older" waters inside this lagoon tend to occur in this location. In the southern region and part of the communication channel, the values varied considerably, mainly due to the tides, alternating between the presence of waters coming from the sea, which are "younger", and waters from the southeast, which are "older". The region identified with the highest W_A values deserves attention, due to its proximity to the east margin, and the influence of the contributions of the urban drainage channels of Maceió, both from the southeast region and also from the south region. As for the waters of these channels, it can be said that they are polluted by the presence of sanitary sewage, as pointed out by the water quality data from IMA-AL, referring to the years 2012, 2013 and 2016. Lira (2019) analyzed the water quality of these channels, and classified them, based on the Water Quality Index (WQI), as bad (values from 41 to 46). In addition, it classified them in Class 3 of water quality, according to CONAMA nº 357. It is mentioned, for example, that the values of Dissolved Oxygen varied between 2.46 and 2.96 mg L^{-1}; Total Nitrogen, from 7.98 to 8.2 mg L^{-1}; Total Phosphorus, from 0.88 to 2.29 mg L^{-1}; and Biochemical Oxygen Demand, from 3.1 to 4.6 mg L^{-1}.

Before discussing the results for the Manguaba L., it is relevant to relate some aspects of the R_T with those of the W_A. While the R_T refers to the time required for the water mass parcels, regardless of their renewal rate, to cross, or not, the control section of the domain of interest, the W_A encompasses the water renewal over time, indicating, on average, how long the waters are within the system. For example, the water masses that started the simulation of the dry season in the position located in front of the mouth of the Silva's Stream, presented R_T of ≈ 80 days. In these 80 days, the environmental forcings promoted the mixing and renewal of these water masses, reaching, for example, at the end of 30 days, a renewal above 50%. The W_A provides results that make it possible to estimate, throughout the simulation, the time needed to renew the water masses that tend to remain inside the lagoons for a longer time.

In the Manguaba L., the lowest W_A at the "Ma North" station was ≈ 2 days, which occurred on the second day of the wet season. In the same station, the average W_A, referring to May, was ≈ 5 days. Note that the monthly mean discharges of the Paraíba do Meio R., in the wet season, were below the historical means, resulting in higher W_A. In the northern region, the renewal was carried out by the Paraíba do Meio R., with the contribution, on a smaller scale, of the urban drainage channels of Pilar. In this region, on the east margin, the water masses with the highest RT were concentrated, with values above 80 days. Through the W_A, it can be said, however, that the waters present on this margin were in the modeling domain for ≈ 9 days during May. At the "Ma Center" station, referring to the same month, the average W_A was ≈ 16 days. Through Figure 13, on the right and above, the reduction of the W_A, in the first days of the simulation is clearly observed. The lowest W_A verified in this station was ≈ 11 days, and it occurred 4 days after the peak discharge of the Paraíba do Meio R. To the south of the lagoon, it was noted that the increase in river discharges negatively affected the renewal, due to a greater attenuation of the tides. In this region, the renewal was provided, on a larger scale, by the Sumaúma R., acting mainly on the west margin and on the communication channels. From the knowledge of the areas most influenced by the waters of the Sumaúma R., it is worth mentioning the water quality of this river. Water quality data from the IMA-AL, referring to the years 2012, 2013 and 2016, reveal the presence of industrial and sanitary effluents from the municipality of Marechal Deodoro at the mouth of this river. Based on these data, the Dissolved Oxygen values varied between 0.9 and 7.1 mg L^{-1}, with an average of 2.80 mg L^{-1}; while those of Ammoniacal Nitrogen, from 0.01 to 0.43 mg L^{-1}, with an average of 0.08 mg L^{-1}; those of Total Phosphorus, from 0.11 to 3.28 mg L^{-1}, with an average of 1.18 mg L^{-1}. For the Biochemical Oxygen Demand, values lower than 2 mg L^{-1} up to a maximum of 21 mg L^{-1} were found.

As can be seen in Figure 14, on the right, the "older" waters, during May, were concentrated between the central and southern regions, especially on the east margin, with a maximum W_A of ≈ 22 days. This result is coherent, since the residual currents, during the wet season, are from north to south, which means that waters in the northern region are "younger", while those between the central and southern regions are the "oldest". At the "Ma South" station, the values varied significantly throughout the simulation, mainly due to river discharges and tides. In this station, in general, the highest W_A occurred in the ebbs of the neap tidal cycles, with the highest presence of "older" waters coming from upstream. The lowest W_A were observed in the floods of the spring tidal cycles, with the presence of "younger" waters, mainly from the Sumaúma R., but also from the sea.

In the dry season, the station "Ma Center" presented a maximum W_A of ≈ 36 days. This means that it is in the vicinity of this region that the "oldest" waters predominate, considering the entire MMELS, as can be seen in Figure 15, on the right. Note that it is not necessarily about the residence of the waters in this region, but rather, that when passing through this place, at a given moment, the waters are already within the modeling domain for, on average, ≈ 36 days. It is also mentioned that for environmental forcings similar to those that occurred in November, it would take a little more than 1 month to renew at least 50% of the waters in the central region. Due to its higher W_A, this region deserves attention, especially the west margin, which can be influenced by polluting loads both upstream and downstream. Therefore, this is a place where water quality monitoring is recommended. At the "Ma North" station, the maximum W_A was ≈ 18 days. This value was close to twice the maximum value reached in the wet season, demonstrating how the reduction in river discharges considerably affected the water renewal in the northern region. In the southern part, the values showed considerable variation over time, for the reasons explained above, with the exception that the “younger” waters in this season are mostly from the sea. Because of this, it is possible to infer that a better water quality tends to occur during the presence of “younger” waters, while the opposite, tend to occur in the presence of “older” waters.

Pinheiro *et al.* (2021), based on Pinheiro (2020), observed that the southeast region of the Mundaú L., both in relation to the wet and dry seasons, presented the highest W_A in this lagoon. In the wet season, with values slightly above 30 days, while in the dry season, slightly above 40 days. For the Manguaba L., in the wet season, the highest W_A occurred in the southern region, with ≈ 52 days, while in the dry season, between the central and southern regions, with 71 days. Some points can be highlighted, which help to explain the higher values found in these studies, compared to this work. The authors admitted an extensive area of oceanic open boundary; however, coastal currents were not considered, which clearly influenced the results, since part of the waters that left the MMELS tended to return to the communication channels/lagoons, instead of being directed along the coast. In addition, in the Manguaba L., the greater tidal attenuation compared to the measured values, in association with the disregard of the Sumaúma R., caused higher WA in the southern region.

3.4. The W_A and the Trophic State Index

In general, based on ANA (2006) and Cotovicz Jr. *et al.* (2012), the input of industrial and domestic effluents is lower in the Manguaba L., compared to Mundaú L. However, due to the hydrodynamic circulation of the Manguaba L., this lagoon tends to accumulate more pollutants than the Mundaú L. As a result, the Manguaba L. has a high trophic state index. Melo-Magalhães *et al.* (2009) found, in a dry season, eutrophic state in the northern and southern regions of Manguaba L., while in the central region, hypertrophic state, based on the concentrations of chlorophyll *a* and total phosphorus. In the wet season, only in the southern region eutrophic state was observed. At Mundaú L., all stations showed hypertrophic state in both seasons. Based on the results of the authors, it can be interpreted that the regions with the highest WA - in Manguaba L., near the central region, and in Mundaú L., the southeast region - had higher total phytoplankton density (cell. L^{-1}), indicating that the WA helps to identify the regions most conducive to more critical trophic states.

The positive correlation between areas that have higher WA and more critical trophic states can also be established from the study by Lins *et al.* (2018). In this, the authors employed remote sensing techniques, together with measured reflectance and chlorophyll *a* data, to estimate the spatial-temporal variability of chlorophyll *a*, as well as the trophic state of MMELS, in the period of 2002 to 2016. It was observed that the trophic state of the Mundaú L. varied between mesotrophic and supertrophic, with an annual predominance of the eutrophic state. It was also found that the region located between the center of the lagoon and its communication channels, presented, in general, the highest mean concentrations of chlorophyll *a* and, therefore, it was the one that presented the highest temporal percentage in the supertrophic state. In the Manguaba L., the situation was more critical, with trophic state varying from eutrophic to hypertrophic. The highest mean concentrations of chlorophyll *a* occurred in the region between the center and the south of the lagoon, which presented the highest temporal percentage in the hypertrophic state. On the other hand, it was found in the northern region the lowest mean concentrations and the predominance of the eutrophic state. Based on this information, it can be said that the WA proved to be, through this study, a CHT capable of providing significant results regarding the mixing and renewal of water masses in different sectors of the lagoons, in addition to indicating the regions with greater possibility of presenting more critical trophic states. Therefore, its application is recommended for CHT analysis.

In summary, based on the results obtained and on the studies from Lima (2017), ANA

(2013), Pinheiro *et al.* (2021), among others, it can be said that the wet seasons, with the recurrence of large river discharges, provide the renewal and exportation of water masses in a much shorter time compared to the dry seasons. Just as the river helps to export pollutants present in the lagoons, it also introduces them, so that, over time, there is no effective improvement in water quality, based on Lins (2017), when she mentions: “During the satellite monitoring period (2002 to 2016), there was no tendency to change the trophic state of the MMELS, indicating that there is a certain resilience of the system and a condition of stability”. Therefore, it is important to reduce the input of pollution from drainage basins, in order to achieve a better water quality in rivers and lagoons. For the Manguaba L., considering the tendency for the accumulation of organic matter and the cycling of nutrients (Costa *et al.*, 2010, Cotovicz Jr. *et al.*, 2012; Lins, 2017), it would be beneficial to increase the water exchange between the lagoon and the sea, helping to export these substances. Such an increase could be made with dredging.

4. CONCLUSIONS

This study reached the proposed objectives, deepening the knowledge about the hydrodynamics and renewal of MMELS waters. The hydrodynamic modeling appropriately represented water level variations measured in the lagoons, in which the great attenuation of the tides was observed, mainly in the Manguaba L., whose average tidal prism corresponded to only 3% of its average volume. The analysis of residual currents clearly indicated the differences in hydrodynamic circulation between the wet and dry season. In the wet season, the residual currents were mostly towards the communication channels, showing how the discharges of the Mundaú and Paraíba do Meio R. strongly influenced the hydrodynamic circulation, especially during peak discharges, as shown in the results of time series of resulting flows and volumes. In the dry season, however, it was possible to verify greater influence of the winds in the induction of currents, through the observation of circulatory cells in the lagoons, one of the most expressive, in the northern region of the Manguaba L. In this region, low currents speed prevailed, as well as in the southeastern region of the Mundaú L. This information was essential to understand the results of the R_T and W_A simulations.

The R_T analysis revealed significant differences between the wet and dry seasons. In the wet season, the peak discharges provided rapid export, mainly in the Mundaú L., where values lower than 2 days were obtained in most of its extension. In the Manguaba L., the maximum river discharge was much lower and it was observed, as a result of the discharges and winds, that the water masses in the northern region, close to the east margin, presented the highest RT, over 80 days. The Mundaú and Paraíba do Meio R. usually promote, during the wet seasons, a great export of pollutants present in the respective lagoons, however, these present, over time, a certain resilience and stability regarding their trophic states. In view of this scenario, it is important to reduce the input of pollution from the drainage basins, in order to achieve a better water quality. In the dry season, the highest R_T in the Mundaú L. occurred in the northwest region, with the same time of the simulation, i.e., 92 days. Then, the region in front of the mouth of the Silva’s Stream, with ≈ 80 days. In the Manguaba L., the northern region was the most critical, with a predominance of R_T equal to the simulation time, i.e., 92 days, with a tendency to much higher values. This region, therefore, is highly vulnerable to the input of pollution, as the pollutants released tend to remain in this portion of the lagoon for a long time, worsening the water quality. Another prominent location was the central region, on the west margin, which, as a result of the hydrodynamic circulation during the dry season, is a place where water masses tend to converge and, therefore, is susceptible to the influence of polluting loads both from upstream and downstream, released on this margin.

The R_T is the most studied CHT of the MMELS, and it is already known which regions typically present, during the dry seasons, the highest R_T values – in Manguaba L., the north region, with R_T usually over 90 days, in a large part of its area; while in Mundaú L., the region between the center and east margin, with R_T usually over 50 days. In order to deepen knowledge about water renewal, through a different perspective, and as yet little-explored in the study region, this work presented the concept and analysis of W_A. For the MMELS, one of the main benefits of using W_A, compared to R_T, is due to the possibility of obtaining more significant results regarding the mixing and water renewal, also indicating how long, on average, the waters are within the modeling domain throughout the simulation. This information cannot be obtained through a map of isolines of R_T, referring to the final instant of the simulation, which only informs the time required for the water masses parcels, regardless of their renewal rate, to cross or not, the control section of the domain of interest. Therefore, it is recommended that W_A be considered in future CHT analyses.

In the wet season, it was found in the Mundaú L. that the highest W_A, i.e., the waters that had been circulating through the lagoon for the longest time, occurred in the southern region and in part of the communication channel, reaching, in May, the maximum value of ≈ 13 days. In the Manguaba L., the "oldest" waters, in the same month, occurred between the central and southern regions, especially on the east margin, with values of ≈ 22 days. This result was fully consistent with the analysis of residual currents, which indicated that the renewal, in general, would occur progressively, from the northern region towards the communication channels. In the dry season, the highest W_A, in the Mundaú L., were found near the southeast region, with a maximum of 29 days, while in the Manguaba L., in the vicinity of the central region, with a value of ≈ 36 days, the highest in the entire MMELS. In both regions, water renewal occurred slowly, in addition, they were confirmed as the places that present the most critical trophic state index, in each lagoon, showing that W_A is a CHT that indicates the regions most conducive to more critical trophic states. These regions deserve attention and, therefore, it is recommended that water quality parameters be monitored.

It is concluded that the use of environmental modeling in MMELS is an indispensable tool to support environmental management. For, in addition to providing relevant information regarding the diagnosis of hydrodynamic circulation and water renewal, it can also be used to predict improvements in water quality, due to the reduction of pollution, as well as interventions in communication channels and inlets, through dredging.

5. REFERENCES

ANA (Brasil). **Atlas esgotos: despoluição de bacias hidrográficas**. Brasília, 2017.

ANA (Brasil). **Coleta e análise da qualidade de sedimentos da Lagoa Mundaú (Maceió/AL)**. Brasília, 2012b.

ANA (Brasil). **Diagnóstico e modelagem hidrodinâmica e de qualidade das águas do Complexo Estuarino da lagoa Mundaú**. Brasília, 2013.

ANA (Brasil). **Levantamento Batimétrico na Lagoa Mundaú**. Brasília, 2012a.

ANA (Brasil). **Monitoramento de qualidade de água na Lagoa Mundaú (Maceió/AL) – Relatório Técnico**. Brasília, 2012c.

ANA (Brasil). **Plano de Ações e Gestão Integrada do Complexo Estuarino-Lagunar Mundaú/Manguaba (CELMM)**. Brasília, 2006.

ANA (Brasil). **Portal Hidroweb.** 2021. Available at: https://www.snirh.gov.br/hidroweb/apresentacao. Access: 2022.

AGUILERA, L.; SANTOS, A. L. F.; ROSMAN, P. C. C. On characteristic hydraulic times through hydrodynamic modeling: discussion and application in Patos Lagoon (RS). **Revista Ambiente & Água**, v. 15, n. 2, p. 2456, 2020. https://doi.org/10.4136/ambi-agua.2456

BARROS, A. H. C.; ARAÚJO FILHO, J. C.; SILVA, A. B.; SANTIAGO, G. A. C. F. **Climatologia do Estado de Alagoas**. Recife: Embrapa Solos, 2012.

BOCANIOV, S. A.; SCAVIA, D. Nutrient Loss Rates in Relation to Transport Time Scales in a Large Shallow Lake (Lake St. Clair, USA-Canada): Insights From a Three-Dimensional Model. **Water Resources Research**, v. 54, n. 6, p. 3825–3840, 2018. https://doi.org/10.1029/2017WR021876

BUCKMANN, M. F. Y. **A persistência do excesso de tensão no fundo como critério de estabilidade hidro-sedimentológica de canais de maré**. 2019. 208 f. Tese (Doutorado em Engenharia Oceânica) - Universidade Federal do Rio de Janeiro, Rio de Janeiro, 2019.

BRASIL. Diretoria de Hidrografia e Navegação – DHN. **Carta Náutica do Porto de Maceió CN Nº 901 e Proximidades do Porto de Maceió CN Nº 920**. Niterói, 1977.

BRITO Jr., A. N.; FRAGOSO Jr., C. R.; LARSON, M. Tidal exchange in a choked coastal lagoon: A study of Mundaú Lagoon in northeastern Brazil. **Regional Studies in Marine Science**, v. 17, p. 133–142, 2018. https://doi.org/10.1016/j.rsma.2017.12.005

COSTA, T. L. F.; ARAUJO, M. P; CARREIRA, R. S.; KNOPPERS B. A. Lipídios como indicadores de fontes e distribuição de matéria orgânica particulada em um complexo estuarino-lagunar tropical (Mundaú-Manguaba, AL). **Química Nova**, v. 33, n. 9, p. 1915-1922, 2010. https://doi.org/10.1590/S0100-40422010000900018

COTOVICZ Jr., L. C.; BRANDINI, N.; KNOPPERS, B. A.; SOUZA, W. F. L.; MEDEIROS, P. R. P. Comparação de Modelos e Índices para Avaliação do Estado Trófico do Complexo Estuarino-Lagunar Mundaú-Manguaba, (AL). **Geochimica Brasiliensis**, v. 26, n. 1, p. 7–18, 2012. http://www.ppegeo.igc.usp.br/index.php/geobras/article/view/10110

COUTINHO, M. K; ASSAD, L. T; NORMANDE, A. C. L; BRANDÃO, T. B. C. **A Cada Lata**: A Extração do Sururu na Lagoa Mundaú - Alagoas. v.6. Brasília: IABS, 2014.

CPRM. **Estudos sobre a instabilidade do terreno nos bairros Pinheiro, Mutange e Bebedouro, Maceió (AL), Ação Emergencial no Bairro Pinheiro**. v.1. Brasília, 2019.

CUNHA, C. L. N.; SCUDELARI, A. C.; SANT’ANA, D. O.; LUZ, T. E. B.; PINHEIRO, M. K. R. Effects on circulation and water renewal due to the variations in the river flow and the wind in a Brazilian estuary lagoon complex. **Revista Ambiente & Água**, v. 16, n. 2, 2021. https://doi.org/10.4136/ambi-agua.2600

DALAZEN, J. P.; CUNHA, C. L. N.; ALMEIDA, R. C. Determinação das taxas de renovação das águas no complexo estuarino de Paranaguá. **Engenharia Sanitária e Ambiental**, v. 25, n. 6, p. 887–899, 2020. https://doi.org/10.1590/S1413-4152202020180019

DANISH HYDRAULIC INSTITUTE – DHI. **MIKE 21 & MIKE 3 Flow Model FM:** Hydrodynamic Module. Short Description. 2021. Available at: https://www.mikepoweredbydhi.com/download/product-documentation Access: 2022.

DELTARES. **Delft-3D-FLOW**. Simulation of multi-dimensional hydrodynamics flows and transport phenomena, including sediments. User Manual. 2021. Available at: https://content.oss.deltares.nl/delft3d/manuals/Delft3D-FLOW_User_Manual.pdf Access: 2022.

DU, J.; SHEN, J. Water residence time in Chesapeake Bay for 1980-2012. **Journal of Marine Systems**, v. 164, p. 101–111, 2016. https://doi.org/10.1016/j.jmarsys.2016.08.011

ELDER, J. W. The dispersion of marked fluid in turbulent shear flow. **Journal of Fluid Mechanics,** v. 5, n. 4, p. 544-560, 1959. https://doi.org/10.1017/S0022112059000374

EMPRESA DE PORTOS DO BRASIL; INSTITUTO NACIONAL DE PESQUISAS HIDROVIÁRIAS. **Relatório da segunda campanha de medições hidráulicas-sedimentológicas do complexo lagunar Mundaú/Manguaba**. Rio de Janeiro: INPH, 1985. (INPH- 73/85. Relatório interno).

GAO, G.; XIA, J.; FALCONER, R. A.; WANG, Y. Modelling Study of Transport Time Scales for a Hyper-Tidal Estuary. **Water**, v. 12, n. 9, p. 2434, 2020. https://doi.org/10.3390/w12092434

GAO, Q.; HE, G.; FANG, H.; BAI, S.; HUANG, L. Numerical simulation of water age and its potential effects on the water quality in Xiangxi Bay of Three Gorges Reservoir. **Journal of Hydrology**, v. 566, p. 484–499, 2018. https://doi.org/10.1016/j.jhydrol.2018.09.033

IBGE. **Censo Demográfico.** 2010. Available at: https://www.ibge.gov.br/estatisticas/downloads-estatisticas.html Access: 2022.

KNOPPERS, B.; KJERFVE, B.; CARMOUZE, J. P. Trophic state and water turn-over time in six choked coastal lagoons in Brazil. **Biogeochemistry**, v. 14, n. 2, p. 149-166, 1991. https://doi.org/10.1007/BF00002903

LARSSON, L.; NILSSON, S. **Hydrodynamic Modeling of the Mundaú-Manguaba Estuarine-Lagoon System, Brazil**. 2014. 85 f. Master thesis (Water Resources Engineering) - Lund University, Lund, 2014.

LIMA, A. C. C. **Condições Hidrodinâmica e estimativas do tempo de residência no Complexo Estuarino Lagunar Mundaú/Manguaba (AL) através de modelagem computacional**. 2017. 102 f. Dissertação (Mestrado em Meteorologia) - Universidade Federal de Alagoas, Maceió, 2017.

LIMA, L. S. **Acoplamento de modelos hidrológicos e hidrodinâmicos para prognóstico ambiental detalhado de longo prazo**. 2016. 144 f. Tese (Doutorado em Engenharia Oceânica) - Universidade Federal do Rio de Janeiro, Rio de Janeiro, 2016.

LINS, R. C. **Avaliação espaço-temporal da clorofila-a em um sistema estuarino-lagunar utilizando sensoriamento remoto e técnicas estatísticas multivariadas**. 2017. 104 f. Tese (Doutorado em Engenharia Civil) - Universidade Federal de Pernambuco, Recife, 2017.

LINS, R. C.; MARTINEZ, J. M.; MARQUES, D. D. M.; CIRILO, J. A.; MEDEIROS, P. R. P.; FRAGOSO Jr., C. R. A Multivariate Analysis Framework to Detect Key Environmental Factors Affecting Spatiotemporal Variability of Chlorophyll-a in a Tropical Productive Estuarine-Lagoon System. **Remote Sensing**, v. 10, n. 6, p. 853, 2018. https://doi.org/10.3390/rs10060853

LIRA, T. K. D. S. **A qualidade da água em riachos do complexo estuarino lagunar Mundaú-Manguaba – CELMM**. 2019. 90 f. Dissertação (Mestrado Profissional em Tecnologias Ambientais) - Instituto Federal de Alagoas, Marechal Deodoro, 2019.

LIU, S.; YE, Q.; WU, S.; STIVE, M. J. F. Wind Effects on the Water Age in a Large Shallow Lake. **Water**, v. 12, n. 5, p. 1246, 2020. https://doi.org/10.3390/w12051246

MACEIÓ. Secretaria de Desenvolvimento Territorial e Meio Ambiente. **Plano de Saneamento Básico do Município de Maceió/AL – PMSB**. Maceió, 2017.

MARSOOLI, R.; ORTON, P. M.; FITZPATRICK, J.; SMITH, H. Residence Time of a Highly Urbanized Estuary: Jamaica Bay, New York. **Journal of Marine Science and Engineering**, v. 6, n. 2, 2018. http://dx.doi.org/10.3390/jmse6020044

MELO-MAGALHÃES, E. M.; MEDEIROS, P. R. P.; LIRA, M. C. A.; KOENING, M. L.; MOURA, A. N. Determination of eutrophic regions on Mundaú/Manguaba lagoons, Alagoas, Brazil, through studies with phytoplanktonic community. **Brazilian Journal of Biology**, v. 69, n. 2, p. 1–10, 2009. https://doi.org/10.1590/S1519-69842009000200006

MONSEN, N. E.; CLOERN, J. E.; LUCAS, L. V.; MONISMITH, S. G. A comment on the use of flushing time, residence time, and age as transport time scales. **Limnology and Oceanography**, v. 47, n. 5, p. 1545–1553, 2002. https://doi.org/10.4319/lo.2002.47.5.1545

NUNES, A; LARSON, M.; FRAGOSO JR., C. R.; HANSON, H. Modeling the salinity dynamics of a choked coastal lagoon and its impact on the Sururu mussel (Mytella falcata) population. **Regional Studies in Marine Science**, v. 45, n. 101807, 2021. https://doi.org/10.1016/j.rsma.2021.101807

OLIVEIRA, A. M.; KJERFVE, B. Environmental Responses of a Tropical Coastal Lagoon System to Hydrological Variability: Mundaú-Manguaba, Brazil. **Estuarine, Coastal and Shelf Science**, v. 37, n. 6, p. 575–591, 1993. https://doi.org/10.1006/ecss.1993.1074

PETROBRAS. **Levantamento Batimétrico na Área da Lagoa Manguaba (AL)**. Salvador, 2011.

PHAM VAN, C.; DE BRYE, B.; DE BRAUWERE, A.; HOITINK, A. J. F.; SOARES-FRAZÃO, S.; DELEERSNIJDER, E. Numerical Simulation of Water Renewal Timescales in the Mahakam Delta, Indonesia. **Water**, v. 12, n. 4, p. 1017, 2020. https://doi.org/10.3390/w12041017

PINHEIRO, M. K. R. **Circulação hidrodinâmica e renovação das águas no complexo estuarino lagunar Mundaú-Manguaba para diferentes configurações de embocaduras**. 2020. 131f. Dissertação (Mestrado em Engenharia Sanitária e Ambiental) – Universidade Federal do Rio Grande do Norte, Natal, 2020.

PINHEIRO, M. K. R.; CUNHA, C. L. N.; LUZ, T.E.B.; SCUDELARI, A. C. Water Renewal in the Mundaú-Manguaba Estuarine-Lagoon Complex (Alagoas, Brazil) under Different inlet configurations. **Revista de Geociências do Nordeste**, v. 7 n. 2, p. 295–306, 2021. https://doi.org/10.21680/2447-3359.2021v7n2ID24914

QI, H.; LU, J.; CHEN, X.; SAUVAGE, S.; SANCHEZ-PÉREZ, J. M. Water age prediction and its potential impacts on water quality using a hydrodynamic model for Poyang Lake, China. **Environmental Science and Pollution Research**, v. 23, n. 13, p. 13327–13341, 2016. https://doi.org/10.1007/s11356-016-6516-5

RIBAS, D. S. L.; JUNKES, J. A.; RODRIGUES, D. F. (Orgs.). **Saúde nunca veio aqui**. Rio de Janeiro: Bonecker, 2019. 108 p.

ROSMAN, P. C. C. Subsídios para modelagem de sistemas estuarinos. *In*: ROSMAN, P. C. C.; ALMEIDA, A. B.; EIGER, S. **Métodos Numéricos em Recursos Hídricos**. 3. ed. Porto Alegre: ABRH, 1997. Cap. 3, p. 238–348.

ROSMAN, P. C. C. (ed.). **Referência Técnica do SisBaHiA®**. Rio de Janeiro: Fundação Coppetec; COPPE/UFRJ, 2021. Avilable at: http://www.sisbahia.coppe.ufrj.br/ Acess: 2022.

ROVERSI, F.; ROSMAN, P. C. C.; HARARI, J. Water renewal analysis of the Santos Estuarine System using computational modeling. **Revista Ambiente & Água**, v. 11, n. 3, p. 566–585, 2016. https://doi.org/10.4136/ambi-agua.1770

SÃO PAULO (Cidade). Superintendência de projetos e de obras. **Diretrizes de Projeto para Estudos Hidrológicos – Método de "I-PAI-WU"**. São Paulo, 1999.

SILVA, L. M. D. **Análise de Circulação Hidrodinâmica e de Qualidade de Água no Sistema Estuarino do Rio Paraíba do Norte, PB**. 2019. 132 f. Dissertação (Mestrado em Engenharia Oceânica). Universidade Federal do Rio de Janeiro, Rio de Janeiro, 2019.

SNIS (Brasil). **24º Diagnóstico dos Serviços de Água e Esgotos – 2018**. Brasília: SNS/MDR, 2019. Available at: http://www.snis.gov.br/diagnostico-anual-agua-e-esgotos/diagnostico-dos-servicos-de-agua-e-esgotos-2018 Access: 2022.

SOUZA, A. P. M. **Avaliação do Efeito do Assoreamento na Hidrodinâmica e no Tempo de Residência de um Complexo Estuarino Lagunar Tropical**. 2017. 51 f. Dissertação (Mestrado em Recursos Hídricos e Saneamento) - Universidade Federal de Alagoas, Maceió, 2017.

TAMANO, L. T. O.; ARAUJO, D. M.; LIMA, B. B. C.; SILVA, F. N. F.; SILVA, J. Socioeconomia e saúde dos pescadores de Mytella falcata da Lagoa Mundaú, Maceió-AL. **Boletim do Museu Paraense Emílio Goeldi. Ciências Humanas**, v. 10, n. 3, p. 699–710, 2015. https://doi.org/10.1590/1981-81222015000300011

TOSIC, M.; MARTINS, F.; LONIN, S.; IZQUIERDO, A.; RESTREPO, J. D. Hydrodynamic modeling of a polluted tropical bay: Assessment of anthropogenic impacts on freshwater runoff and estuarine water renewal. **Journal of Environmental Management**, v. 236, p. 695–714, 2019. https://doi.org/10.1016/j.jenvman.2019.01.104

ZHAO, F.; ZHAN, X.; XU, H.; ZHU, G.; ZOU, W.; ZHU, M. *et al.* New insights into eutrophication management: Importance of temperature and water residence time. **Journal of Environmental Sciences**, v. 111, p. 229–239, 2021. https://doi.org/10.1016/j.jes.2021.02.033

SUPLEMENTARY MATERIAL

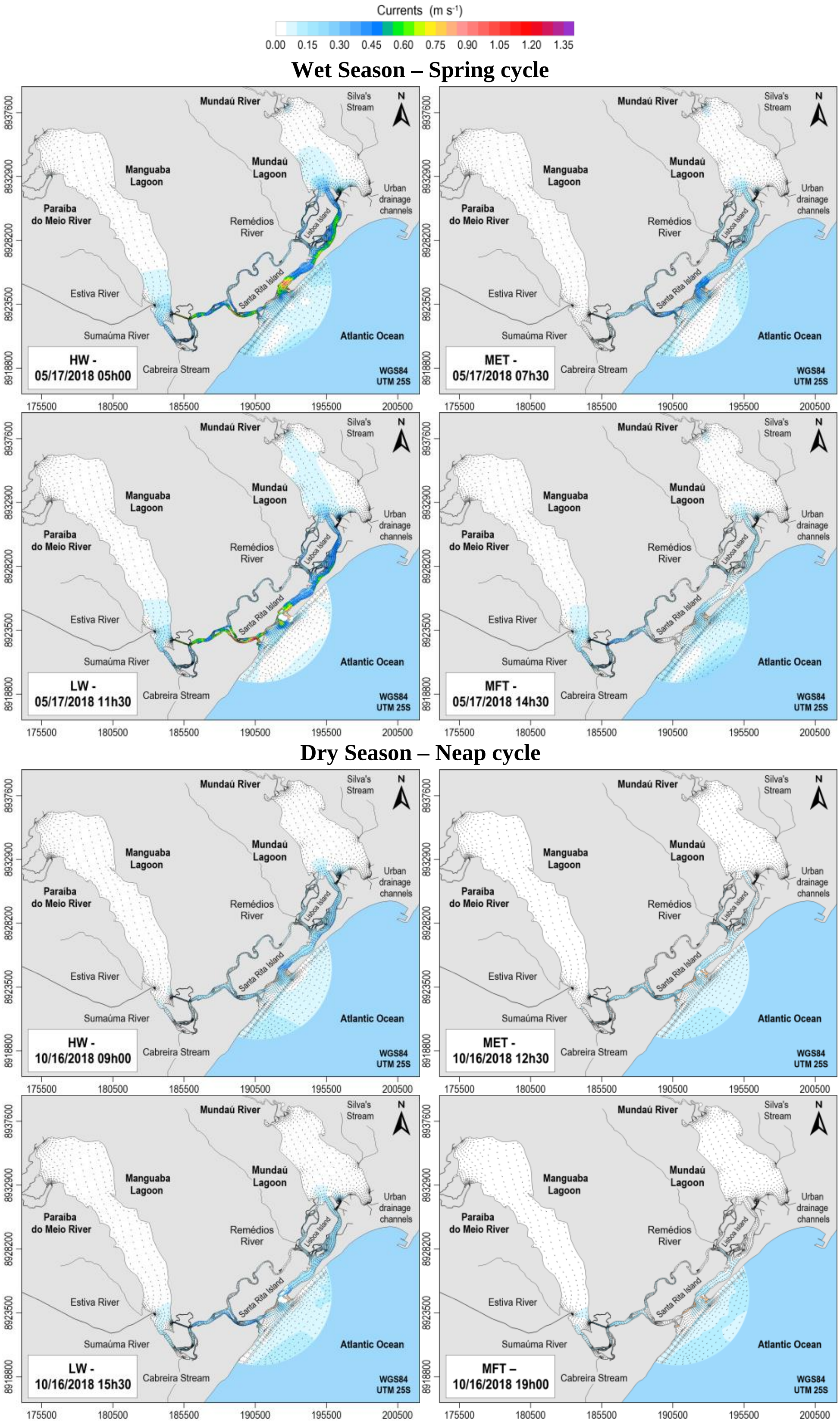

Annex I. Characterization of hydrodynamic circulation patterns through maps of isolines and vectors of currents (average in the water column). Note that the vectors have the same length.